1964

On the theory and design of semiconductor diode parametric amplifiers

Richard A. Stanley
Lehigh University

ON THE THEORY AND DESIGN OF SEMICONDUCTOR DIODE PARAMETRIC AMPLIFIERS - by Richard A. Stanley

Abstract

A theoretical and experimental study of a nondegenerate parametric amplifier using a semiconductor varactor diode is performed.

The basic theory of the semiconductor-diode parametric amplifier is presented. It is shown that the diode and idler together can be considered equivalent to a negative admittance whose value depends on the pump power. Relations for gain, bandwidth, and noise figure are derived, and it is shown that the most important single parameter governing amplifier performance is the dynamic quality factor of the diode. This theoretical part represents a consolidation of much earlier material which has appeared, widely scattered, in the literature.

A coaxial configuration for a 4 gc. parametric amplifier is designed and built. Methods for adjusting the resonance of the amplifier cavities and optimizing the noise performance by plotting the input impedance locus are described. The latter predicts a noise figure of 4.4 db. A gain of 4.8 db. is observed without final optimization of the signal circuit and pump injection. Suggestions are made for further work on this amplifier.

ON THE THEORY AND DESIGN OF SEMICONDUCTOR DIODE PARAMETRIC AMPLIFIERS

by
Richard Alan Stanley

A THESIS

Presented to the Graduate Faculty

of Lehigh University

in Candidacy for the Degree of

Master of Science

Lehigh University

1964

This thesis is accepted and approved in partial fulfillment of the requirements for the degree of Master of Science.

May 22, 1964
(date)

Nikolai Eberhardt
Professor in Charge

John Karakash
Head of the Department
of Electrical Engineering

Acknowledgements

The opportunity to perform this work was provided by the National Aeronautics and Space Administration, whose assistance is gratefully acknowledged.

The writer is indebted to the Professor in Charge of this project, Dr. Nikolai Eberhardt, for his assistance in the preparation and reading of this paper. It is doubtful that this work could have been accomplished without his help and supervision.

Credit is also due the many persons at the Bell Telephone Laboratories, International Telephone and Telegraph Company and Western Electric Company, who generously lent us certain badly needed pieces of equipment. Particular thanks are due the Western Electric Company, who supplied the microwave diode used in this amplifier.

The assistance of Lieutenant Martin C. Faga, USAF, whose participation in the passive measurements section of this paper was invaluable, is sincerely appreciated.

The writer's wife deserves particular credit, both for typing the manuscript and for the moral encouragement which made it possible.

Table of Contents

List of Figures

ON THE THEORY AND DESIGN OF SEMICONDUCTOR DIODE PARAMETRIC AMPLIFIERS - by Richard A. Stanley

Abstract

A theoretical and experimental study of a nondegenerate parametric amplifier using a semiconductor varactor diode is performed.

The basic theory of the semiconductor-diode parametric amplifier is presented. It is shown that the diode and idler together can be considered equivalent to a negative admittance whose value depends on the pump power. Relations for gain, bandwidth, and noise figure are derived, and it is shown that the most important single parameter governing amplifier performance is the dynamic quality factor of the diode. This theoretical part represents a consolidation of much earlier material which has appeared, widely scattered, in the literature.

A coaxial configuration for a 4 gc. parametric amplifier is designed and built. Methods for adjusting the resonance of the amplifier cavities and optimizing the noise performance by plotting the input impedance locus are described. The latter predicts a noise figure of 4.4 db. A gain of 4.8 db. is observed without final optimization of the signal circuit and pump injection. Suggestions are made for further work on this amplifier.

I. Introduction

As man's interest in communication extends over greater distances than ever before, the ability to detect extremely weak signals becomes more and more important. The obvious solution of increasing transmitter power in order to guarantee consistent communications is a luxury generally unavailable to the designer of missle or aircraft-carried equipment, due to severe limitations of space and weight; and transmitter considerations are certainly of no more than academic interest to the radio-astronomer. Thus, it has become necessary to develop an entire family of devices capable of amplifying extremely weak signals to a level where they can be operated upon by more conventional circuitry. One such device is the parametric amplifier, which is the subject of this paper.

It is well-known that the minimum threshold signal which may be usably amplified by a device is a function of the noise generated within the device itself. While it can be shown that a noise-free device is both theoretically and practically impossible to construct, there is no limitation on how closely the minimum may be approached. The maser is presently the lowest-noise amplifier available, but this device must be operated at very low temperatures, and is quite complex. The parametric amplifier, however, while being only slightly inferior to the maser with respect to inherent noise, possesses the advantage of simplicity and the capability of operation at either room or liquid helium temperatures, as the situation may require. For this reason, it is a device of considerable practical importance.

As is the case with most microwave devices, an exact analysis of the parametric amplifier is virtually impossible because of the complexity of the problem. It is possible, however, to reduce the scope of the problem without seriously limiting the generality of the results by use of a series of excellent approximations. This procedure will be followed herein.

It is the purpose of this paper to present in unified form the essence of the material which has been presented on the parametric amplifier, and to describe the experimental evaluation of a device of rather novel design. To accomplish this, the paper will be divided into three basic sections, the first of which will concentrate on developing the theory of operation of the parametric amplifier, with an eye toward producing results potentially useful in the design of such a device. The methods of analysis will generally be those outlined in several places by Heffner and Wade, Blackwell, Kotzebue, Uenohara, and Rowe.

The second section of the paper will be devoted to the design of the actual amplifier, assuming the configuration suggested to the writer by Dr. Nikolai Eberhardt, of Lehigh University.

The third major part of this presentation will be concerned with the experimental evaluation of parametric amplifiers in general, and the one of section two in particular. It will consider the theory and performance of measurements outlined by Uenohara and Kurokawa, as well as several experimental techniques utilized at Lehigh University in the testing of the amplifier described below.

It is hoped that this paper will serve to unify the basic theory of operation and measurement of parametric devices, as well as providing an insight into how to -- or how not to -- design such a device.

II. Theory of Parametric Amplifiers

1. The Manley-Rowe Equations

The principle of parametric amplification is not new; it was proposed for mechanical systems over a century ago[1,2,3]. However, it has recently been shown[4] that there exists a set of general energy relations for such nonlinear systems, and we shall derive them at this point[5,6]. These equations will prove invaluable in the discussion of the parametric amplifier.

Let us assume a system of the general form of Figure 1. The generators represent those frequencies at which power is supplied; they are set equal to zero if power is not supplied to the nonlinear element at that frequency. Let us also assume the nonlinear element to be capacitive, having characteristics of the form:

$$v = f(q) \tag{1}$$

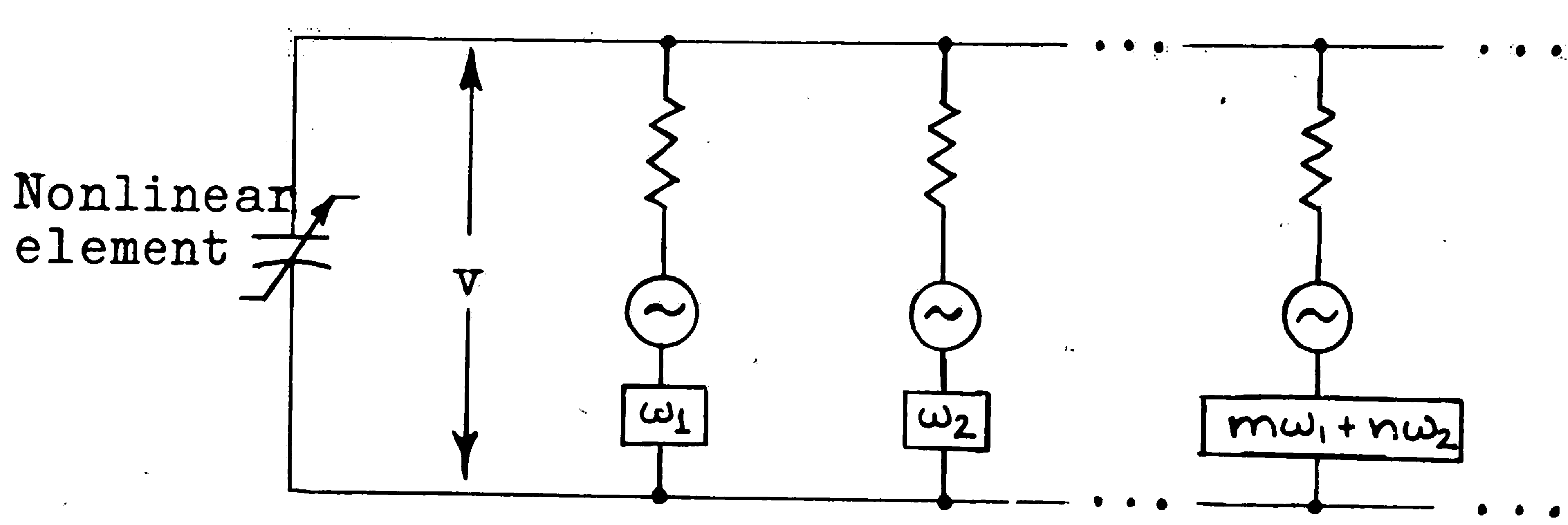

Figure 1. General non-linear circuit for Manley-Rowe derivation.

Assume that power is delivered at only ω_1 and ω_2. We know from the general theory of nonlinear devices that if power is supplied to them at two different frequencies,

ω_1 and ω_2, sum and difference terms involving the fundamentals and their harmonics will be generated, yielding the general form $m\omega_1 + n\omega_2$, where m and n are positive or negative integers. This fact is commonly used in the design of mixer circuits, and it is widely known that such a charge flow is expressable by a double Fourier series:

$$q = \sum_{m=-\infty}^{+\infty} \sum_{n=-\infty}^{+\infty} Q_{mn} e^{j(m\omega_1 t + n\omega_2 t)} \tag{2}$$

Since q is real, it is required that

$$Q_{mn} + Q^*_{-m,-n} \tag{3}$$

The current through the capacitor is readily found:

$$i = \frac{dq}{dt} = \sum_{m=-\infty}^{+\infty} \sum_{n=-\infty}^{+\infty} I_{mn} e^{j(m\omega_1 t + n\omega_2 t)} \tag{4}$$

where $$I_{mn} = j(m\omega_1 + n\omega_2)Q_{mn} = I^*_{-m,-n} \tag{5}$$

Since from (1) the voltage may be expressed as a function of q, it may also be expressed as a function of $(m\omega_1 + n\omega_2)$ in a double Fourier series:

$$v = \sum_{m=-\infty}^{+\infty} \sum_{n=-\infty}^{+\infty} V_{mn} e^{j(m\omega_1 t + n\omega_2 t)} \tag{6}$$

where $$V_{mn} = \frac{1}{4\pi^2} \int_0^{2\pi} \int_0^{2\pi} v e^{-j(m\omega_1 t + n\omega_2 t)} \tag{7}$$

Using elementary circuit theory, the average power flow into the diode at frequency $\pm|m\omega_1 + n\omega_2|$ is given by

$$P_{mn} = 2\mathrm{Re}(V_{mn} I^*_{mn}) = -2(m\omega_1 + n\omega_2)\mathrm{Re}(jV_{mn}Q^*_{mn}) \tag{8}$$

Likewise, $P_{-m,-n} = 2\mathrm{Re}(V_{-m,-n}I^{*}_{-m,-n}) = 2\mathrm{Re}(V^{*}_{mn}I_{mn})$ (9)

$$= 2\mathrm{Re}(V_{mn}I^{*}_{mn}) = P_{mn}$$

Due to conservation of energy, the net average power flow into the capacitor must be zero if it is a pure reactance, thus

$$\sum_{m=-\infty}^{+\infty} \sum_{n=-\infty}^{+\infty} P_{mn} = 0 \tag{10}$$

Multiplying and dividing each term by its frequency,

$$\sum_{m=-\infty}^{+\infty} \sum_{n=-\infty}^{+\infty} (m\omega_1 + n\omega_2)\frac{P_{mn}}{(m\omega_1 + n\omega_2)} = 0 \tag{11}$$

$$\omega_1 \sum_{m=-\infty}^{+\infty} \sum_{n=-\infty}^{+\infty} \frac{mP_{mn}}{m\omega_1 + n\omega_2} + \omega_2 \sum_{m=-\infty}^{+\infty} \sum_{n=-\infty}^{+\infty} \frac{nP_{mn}}{m\omega_1 + n\omega_2} = 0$$

The first double sum in (11) may be rewritten in this manner:

$$\sum_{m=-\infty}^{+\infty} \sum_{n=-\infty}^{+\infty} \frac{mP_{mn}}{m\omega_1 + n\omega_2} = \sum_{n=-\infty}^{+\infty} \left[\sum_{m=-\infty}^{0} \frac{mP_{mn}}{m\omega_1 + n\omega_2} + \sum_{m=0}^{+\infty} \frac{mP_{mn}}{m\omega_1 + n\omega_2} \right]$$

$$= \sum_{n=-\infty}^{+\infty} \left[\sum_{m=0}^{+\infty} \frac{-mP_{-m,-n}}{-m\omega_1 - n\omega_2} + \sum_{m=0}^{+\infty} \frac{mP_{mn}}{m\omega_1 + n\omega_2} \right]$$

$$= 2 \sum_{m=0}^{+\infty} \sum_{n=-\infty}^{+\infty} \frac{mP_{mn}}{m\omega_1 + n\omega_2} \tag{12}$$

where the results of (9) have been used. An exactly similar manipulation of the second double sum allows (11) to be rewritten:

$$\omega_1 \sum_{m=0}^{+\infty} \sum_{n=-\infty}^{+\infty} \frac{mP_{mn}}{m\omega_1 + n\omega_2} + \omega_2 \sum_{m=-\infty}^{+\infty} \sum_{n=0}^{+\infty} \frac{nP_{mn}}{m\omega_1 + n\omega_2} = 0 \tag{13}$$

Since neither ω_1 nor ω_2 is zero, equation (13) will obtain if and only if the coefficients of ω_1 and ω_2 are separately equal to zero for all ω_1 and ω_2. Thus:

$$\sum_{m=0}^{+\infty} \sum_{n=-\infty}^{+\infty} \frac{mP_{mn}}{m\omega_1 + n\omega_2} = 0$$
$$\sum_{m=-\infty}^{+\infty} \sum_{n=0}^{+\infty} \frac{nP_{mn}}{m\omega_1 + n\omega_2} = 0 \qquad (14)$$

Equations (14) are the Manley-Rowe relations, which relate power flow in most nonlinear parametric systems. Note that their derivation utilized the assumption of a lossless nonlinear capacitor, a condition not attainable in practice. For this reason, these equations will not give exact results in actual devices, but serve to establish the theoretical limits of performance.

It should be observed that these equations have not been derived using a general nonlinear element, and for this reason, their use is not justified until their validity has been demonstrated for the case considered. This paper will concern itself only with devices utilizing capacitance, however, so the foregoing derivation is sufficient.

Note also that no linearization has been effected; these relations are not bound to consideration of small-signal phenomena.

The Manley-Rowe relations have not been shown to be true for a linear, time-varying capacitance. That they are indeed valid for this case can be shown by expanding the charge flow in series form:[5]

$$q = \sum_{0}^{\infty} a_n (V - V_{dc})^n$$

where V_{dc} is the DC bias voltage.

Introducing the definition of capacitance:

$$C(V) = \frac{dq}{dv} = \sum_{1}^{\infty} a_n n (V - V_{dc})^{n-1} \tag{15}$$

Let $V - V_{dc} = V_o \cos \omega t$, then

$$C(V) \rightarrow C(t) = \sum_{1}^{\infty} a_n n \left[\frac{V_o}{2}\right]^{n-1} (e^{j\omega t} + e^{-j\omega t})^{n-1}$$

$$= \sum_{-\infty}^{\infty} C_n e^{jn\omega t} \tag{16}$$

where the C_n's consist of the appropriate constants a_n, n, and V_o.

Equation (16) shows that the nonlinear capacitor can be represented by a time-varying linear capacitor. Assuming a small voltage variation, the series expansion gives

$$C(t) \approx C_o + C_1 \cos(\omega t + \phi) \tag{17}$$

where $C_1 \ll C_o$. We shall use equations (14) and (17) in much of the following work.

The usefulness of equations (14) will soon become apparent. For example, suppose we allow power to flow at three frequencies: ω_1, ω_2, and ω_3, where $\omega_3 = \omega_1 + \omega_2$. Then equations (14) reduce to

$$\frac{P_1}{\omega_1} + \frac{P_3}{\omega_3} = 0 \tag{18a}$$

$$\frac{P_2}{\omega_2} + \frac{P_3}{\omega_3} = 0 \tag{18b}$$

If power is delivered to the nonlinear element at ω_3, both ω_1 and ω_2 must be negative; i.e. power is supplied by the nonlinear element at those frequencies. As we have not postulated the existence of a generator of frequency ω_1 or ω_2, it is apparent that this device is capable of supplying power at ω_1 with no external source at that frequency. In other words, it can oscillate.

The behavior described above is that of a regenerative device, and for that reason such a parametric circuit is known as a negative-resistance parametric amplifier. There are other types of parametric amplifiers, some involving frequency conversion, but the sole concern here will be with the negative-resistance device with input and output on the same frequency.

2. Equivalent Circuit of the Parametric Amplifier

It is the purpose of any equivalent circuit to present a description of the device at hand which accurately represents its behavior, and which is capable of solution by the methods of circuit analysis. We will demonstrate an equivalent circuit for the parametric amplifier which not only describes its theoretical behavior but accounts for certain effects inescapable in practice, such as losses.

In general, a semiconductor diode is used as the parametric element. When reverse biased, the junction and diffusion capacitances are generally of the order of a few tenths of a picofarad. This capacitance is easily varied in time by varying the voltage across the diode at an ac rate, giving the desired time-varying capacitance. The only serious limitation to the use of such a diode is its series resistance, which is composed primarily of the ohmic resistance of the semi-conductor material and the contacts made to it. This resistance is generally of the order of one or two ohms. The junction resistance (which shunts the capacitance of the junction) is very large in the back-biased state, and can be neglected, giving the diode equivalent circuit of Figure 2.

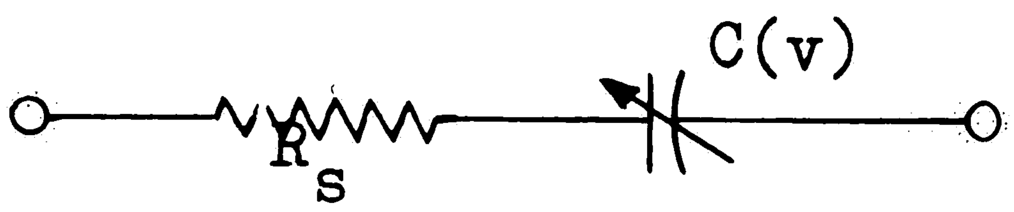

Figure 2. Equivalent circuit of diode.

As a guide to diode selection, many "figures of merit" have been proposed. Common sense is a good guide here; intuitively, we would desire R_s to be small in order to minimize losses and thermal heating. Another quantity of interest is the diode zero bias cutoff frequency, ω_c, defined by

$$\omega_c = \frac{1}{R_s C_o} \qquad (19)$$

where ω_c = cutoff frequency

C_o = diode capacitance for zero DC bias

R_s = diode series resistance

A very useful "quality factor" is then given by the ratio of ω_c to the signal frequency. Uenohara has shown that when this ratio is less than 2.0, amplification with the diode is impossible[7]. Thus, the higher the quality factor, the "better" the diode.

The operation of the parametric amplifier may be represented quite accurately by the equivalent circuit of Figure 3.

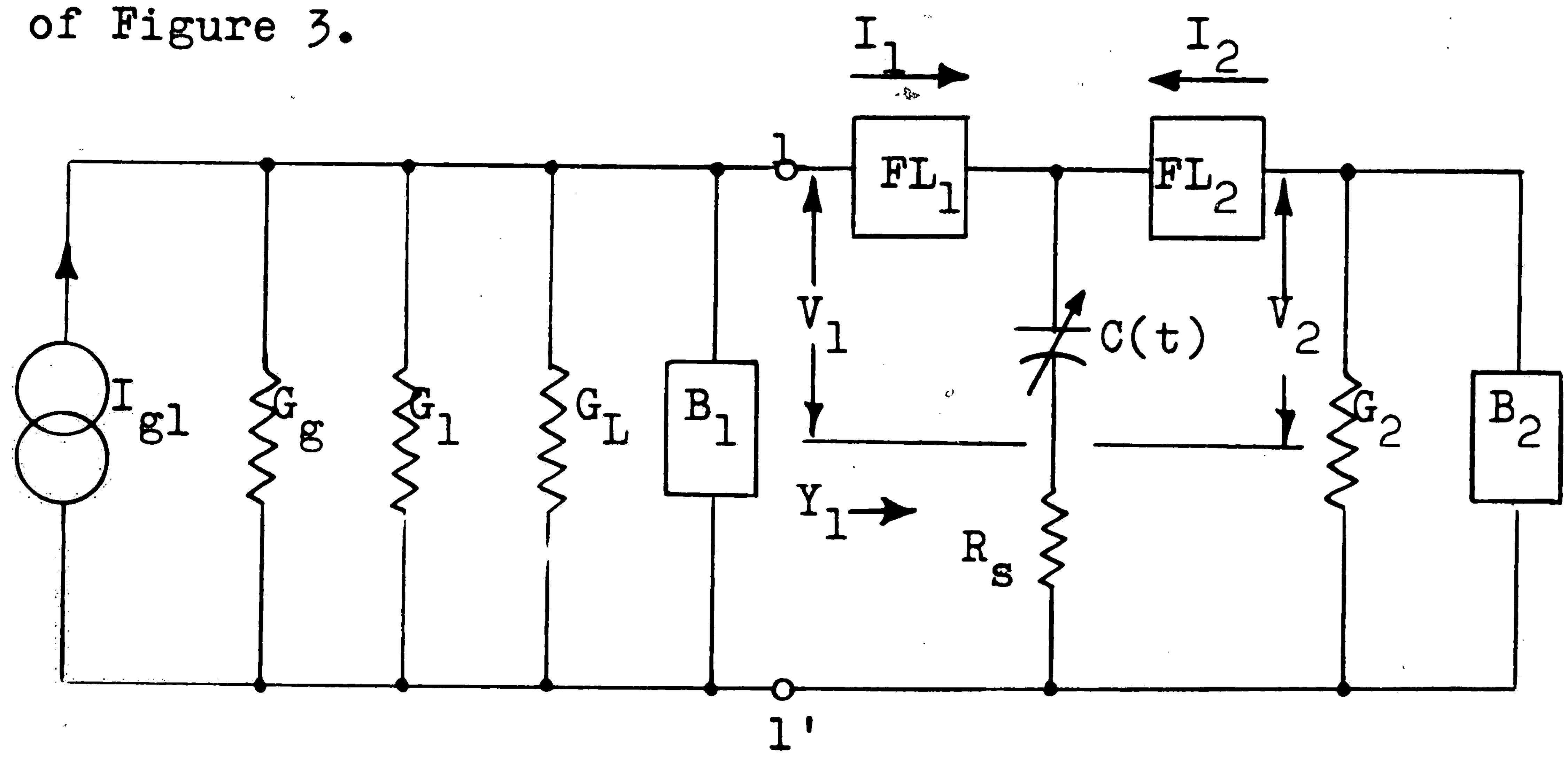

I_{gl} = source at ω_1
G_g = source conductance
G_1 = signal circuit loss conductance
G_L = load conductance
R_s = diode loss resistance
G_2 = idler circuit loading
B_1, B_2 = susceptances of signal and idler circuits
FL_1, FL_2 = ideal filters for frequencies ω_1 and ω_2, respectively. $Z = \infty$ at all other frequencies
$C(t)$ = $C_o + C_3 \sin(\omega_3 t + \phi_3)$; $C_o \gg C_3$
ω_3 = $\omega_1 + \omega_2$
ϕ_3 = arbitrary phase constant

Figure 3. Equivalent circuit and nomenclature of parametric amplifier.

In a circuit such as the above, the following terminology is usually applied to the various frequencies:

ω_1 = signal frequency

ω_2 = idler frequency

ω_3 = pump frequency

In addition, such a circuit represents a single-sideband device, since power is removed only at ω_1. If power were taken out at both ω_1 and ω_2, it would be denoted a double-sideband amplifier. While the latter situation is of limited use in communications systems, it is often used in radioastronomy. Double-sideband operation will not be analyzed here.

Although provision has been made for representing resistive losses in the tuned circuits, in any well designed amplifier they are small compared to R_s, and thus can be neglected in practice. In the same vein, while it is obvious that ideal filters cannot be built, the tuned circuit Q's available at microwave frequencies allow them to be very closely approximated.

3. Analysis of the Two-Tank Amplifier

Using the equivalent circuit of Figure 3, it is possible to obtain virtually all of the significant operating conditions for the parametric amplifier. We shall first determine the conductance presented to the input circuit, and show that it is indeed negative under certain conditions. We shall evaluate the gain and bandwidth of the amplifier from this result, and then formulate expressions which describe the noise performance to be expected. Many such analyses have been made by others, but it is hoped that here the best features of several of these may be utilized in the interests of clarity.

Referring to Figure 3, we see that because of the filters, only voltage of frequencies ω_1 and ω_2 may develop across C(t). This tacitly assumes that all harmonics and intermodulation products are open-circuited. To reduce the calculations to reasonable proportions, and to assure proper operation of the amplifier, it is necessary to assume that the harmonics are disposed of. However, one might just as easily assume them short-circuited, if R_s is sufficiently small. Fortunately, the choice is not critical, for Blackwell and Kotzebue have shown[6] by using the generalized admittance matrix of the diode that essentially the same results obtain whichever approximation is made, provided that the harmonics are actually prevented from reaching the diode by one means or another. This result allows us to proceed under the open-circuit assumption with the assurance that our results will be general.

From the above discussion, the total voltage across C(t) is the sum of the voltages at each and every permitted frequency:

$$V_c = V_1 \sin(\omega_1 + \phi_1) + V_2 \sin(\omega_2 t + \phi_2) \qquad (20)$$

We can incorporate the susceptance of C_o into B_1 and B_2, as C_o serves only as a fixed capacitive loading on the tank circuits. Notice that because of the action of the filters, I_1 and I_2 can contain only components of ω_1 and ω_2, respectively. By definition, under the sign conventions of Figure 3,

$$I_1 = -\frac{d}{dt}(CV_1)$$

which leads to (after Heffner and Wade)[8]:

$$I_1 = \frac{\omega_1 C_3}{2} V_2 \sin(\omega_1 t + \emptyset_3 - \emptyset_2)$$

$$= \mathrm{Re}\left(-j\frac{\omega_1 C_3}{2} V_2 e^{j(\emptyset_3-\emptyset_2)} e^{j\omega_1 t}\right) \qquad (21)$$

and similarily

$$I_2 = \frac{\omega_2 C_3}{2} V_1 \sin(\omega_2 t + \emptyset_3 - \emptyset_1)$$

$$= \mathrm{Re}\left(-j\frac{\omega_2 C_3}{2} V_1 e^{j(\emptyset_3-\emptyset_1)} e^{j\omega_2 t}\right) \qquad (22)$$

Using (21), we can now calculate the effective admittance presented to the generator and input circuit at terminals 1-1'.

$$\overline{Y}_1 = \frac{\overline{I}_1}{\overline{V}_1} = \frac{-j(\omega_1 C_3/2) V_2 e^{j(\emptyset_3-\emptyset_2)} e^{j\omega_1 t}}{jV_1 e^{j\emptyset_1} e^{j\omega_1 t}}$$

$$= -\frac{\omega_1 C_3}{2} \frac{V_2}{V_1} e^{j(\emptyset_3-\emptyset_2-\emptyset_1)} \qquad (23)$$

From (23), we see that Y_1 is negative, and dependent on the amplitude of V_2. The admittance of the idler circuit is readily seen to be

$$Y_2 = G_2 + jB_2 \qquad (24)$$

and by a procedure exactly analogous to that used in finding (23), we may write

$$Y_2 = \frac{-I_2}{V_2} = \frac{j(\omega_2 C_3/2)V_1 e^{j(\phi_3-\phi_1)} e^{j\omega_2 t}}{jV_2 e^{j\phi_2}\, e^{j\omega_2 t}}$$

$$= \frac{\omega_2 C_3}{2} \cdot \frac{V_1}{V_2}\, e^{j(\phi_3-\phi_2-\phi_1)} \qquad (25)$$

Note that Y_2 is a real admittance, and thus positive, while Y_1 is an <u>effective</u> admittance, which may or may not be positive. Rearranging (25), we have

$$\frac{\omega_2 C_3}{2Y_2^*} = \frac{V_2}{V_1}\, e^{j(\phi_3-\phi_2-\phi_1)} \qquad (26)$$

Substituting (26) into (23):

$$Y_1 = -\frac{\omega_1 \omega_2 C_3^2}{4Y_2^*} \qquad (27)$$

Equation (27) is the desired description of the admittance seen looking into terminals 1-1'. Since the derivation assumed nothing about the origins of the voltages V_1 and V_2, equation (27) is perfectly general -- it applies whether the device is amplifying or oscillating. The value of Y_1 is essentially determined by C_3 and Y_2^*, since in practice ω_1 and ω_2 are fixed. This allows the gain of the device to be varied by varying C_3, which is done by changing the pump power. It is of considerable importance that Y_1 does not depend on the phase of any of the alternating voltages applied to the capacitor. If this were not so (and it is not for degenerate parametric amplifiers), it would be necessary to know the phase of the signal relative to the pump, which would render the device useless for general communications purposes.

The existence of (27) allows us to replace everything to the right of terminals 1-1' in Figure 3 by Y_1. This replacement greatly simplifies our calculations, as will be seen in the development of gain and bandwidth relations.

4. Gain Relations

The susceptances B_1 and B_2 have been implicitly assumed to represent lossless parallel resonant circuits with resonant frequencies ω_1 and ω_2 in the preceding work. (If this were not true, no voltages at ω_1 or ω_2 could exist in either the signal or idler circuits). It is convenient to redefine the resonant frequencies of the signal and idler circuits as Ω_1 and Ω_2, where

$$\begin{aligned} \Omega_1 &\approx \omega_1 \\ \Omega_2 &\approx \omega_2 \end{aligned} \tag{28}$$

In the event that $\omega_1 = \Omega_1$ and $\omega_2 = \Omega_2$, we know that $B_1 = B_2 = 0$, and $Y_2^* = G_2$. Equation (27) may then be written

$$-G = -\frac{\omega_1\omega_2 C_3^2}{4G_2} \tag{29}$$

This is the effective admittance for mid-band gain calculations. Figure 4 is the equivalent circuit at resonance.

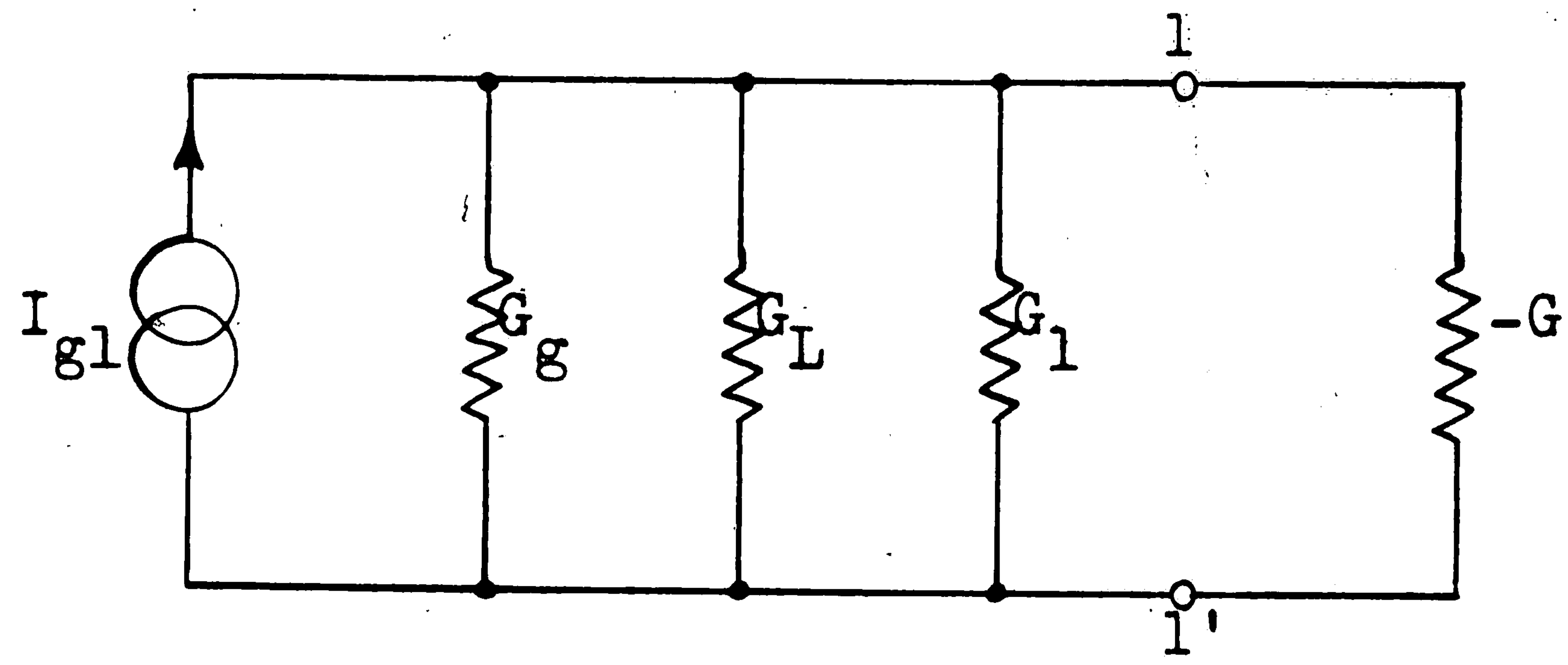

Figure 4. Equivalent circuit of parametric amplifier at resonance.

Transducer gain is defined as the ratio of power dissipated in G_1 to the available power at ω_1. From basic circuit theory,

$$g^2 = \frac{\left[I_{G1}/(G_g+G_L+G_1-G)\right]^2 G_L}{I_G^2/4G_g} = \frac{4G_gG_L}{(G_g+G_L+G_1-G)^2}. \quad (30)$$

It is evident from (30) that for large gain $G \approx (G_g+G_L+G_1)$. It is also evident that such a condition is potentially unstable, for even a slight shift in G could realize the condition for infinite gain, and hence oscillation. Device stability requires, among other things, considerable amplitude stability in the pump source.

Although (30) is perfectly correct, it would be nice if it explicitly included the losses due to R_s. It can be shown[5,7] that R_s may be moved into the external tanks as a shunt conductance of magnitude $(Q_o^2R_s)^{-1}$, provided Q_o is large, where Q_o is the diode static quality factor, and is defined by

$$Q_o = \frac{1}{\omega C_o R_s}. \quad (31)$$

Because of the filters, the transformed R_s must appear separately in the signal and idler tanks to account for the loading effect on these tanks. The transformed equivalent circuit is shown in Figure 5.

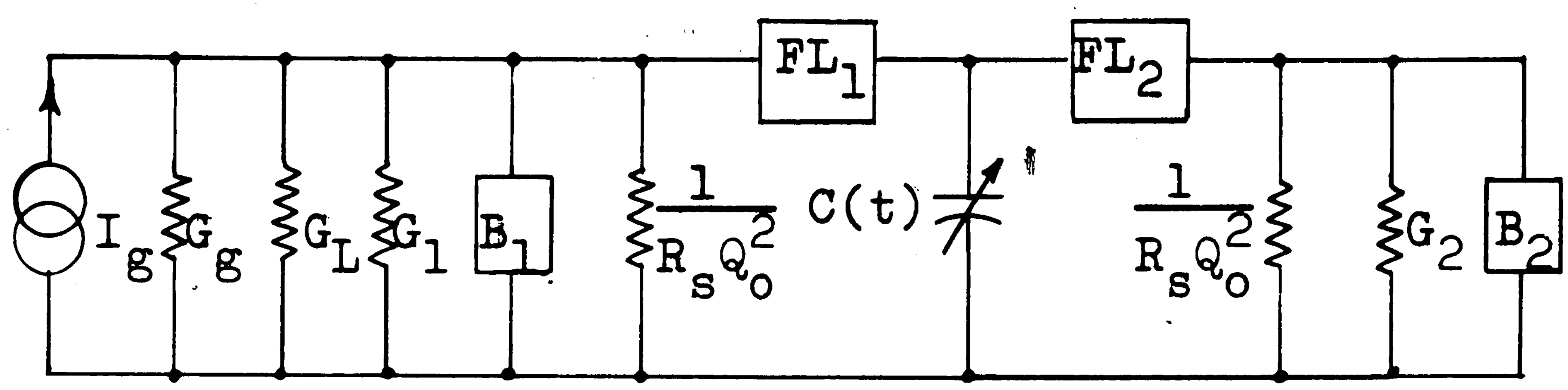

Figure 5. Equivalent circuit of the parametric amplifier with R_s transformed to the external circuit.

From Figure 5, we can readily absorb $\frac{1}{R_s Q_o^2}$ into G_1 and G_2, with the result that

$$G_1' = G_1 + \frac{1}{Q_o^2 R_s}$$
$$G_2' = G_2 + \frac{1}{Q_o^2 R_s} \tag{32}$$

We may now everywhere replace G_1 by G_1', G_2 by G_2', and R_s by zero in Figure 3. This will not change any of our results, but allows us to more readily see the effect of R_s. In particular, note that the value of R_s places a lower limit on the idler loading; this will prove to be significant.

An amplifier with the arrangement of Figure 5, where the load and signal admittances are directly in parallel is known as a transmission-type amplifier.

The parametric amplifier may be considerably stabilized if the signal is injected and removed by means of a circulator. The equivalent circuit at midband is shown in Figure 6, assuming that any circulator losses are absorbed into G_1'.

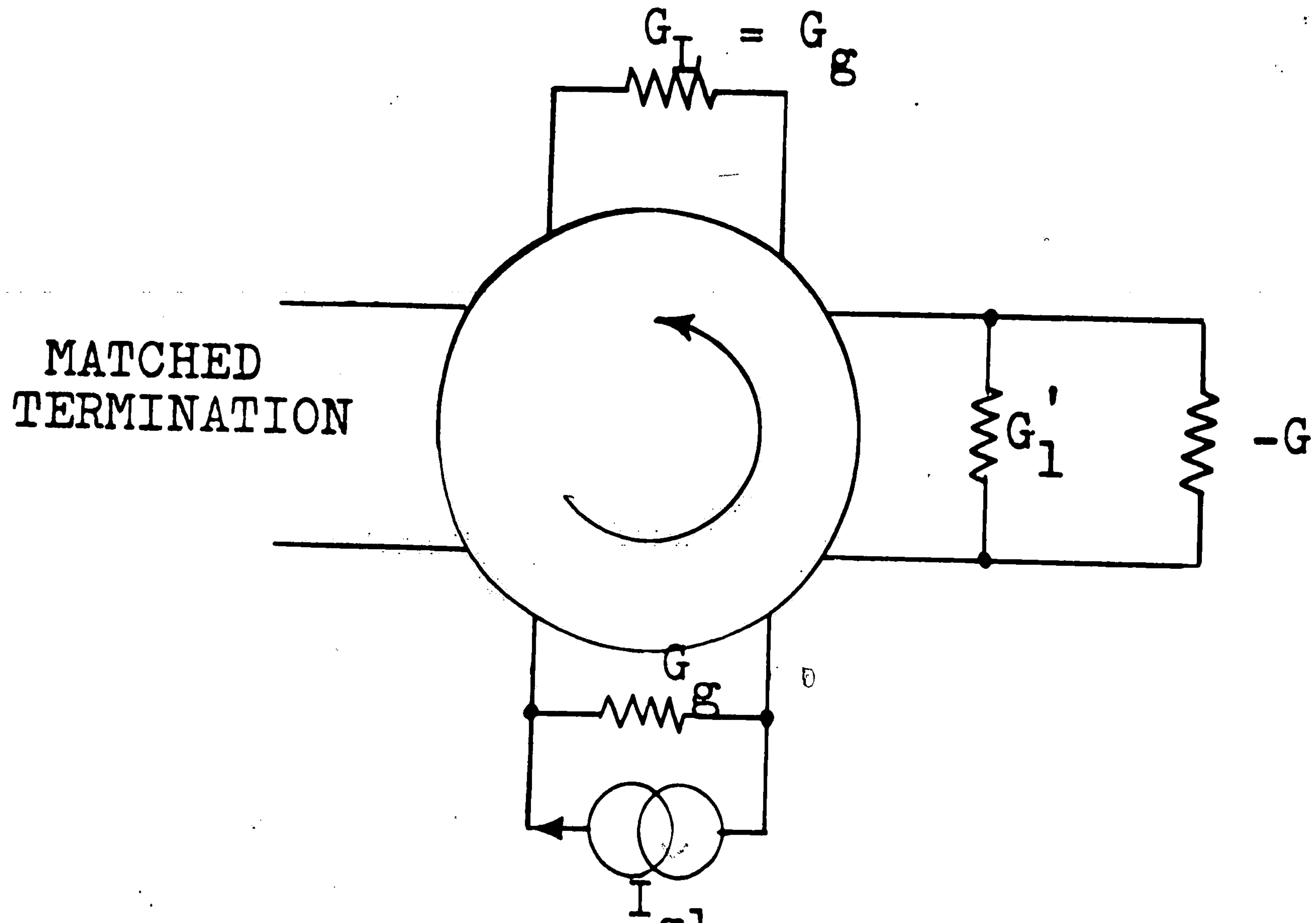

Figure 6. Negative-resistance parametric amplifier using a circulator.

The device in Figure 6 is a reflection-type amplifier, and its power gain is simply the ratio of reflected to incident power. If the input and output impedances are equal, the power gain is just the square of the amplifier voltage-reflection coefficient.

$$g^2 = \rho^2 = \left[\frac{Z_L - Z_o}{Z_L + Z_o}\right]^2 = \left[\frac{G_g - (G_1' - G)}{G_g + (G_1' - G)}\right]^2 \tag{33}$$
$$= \left[\frac{(R_1' - R) - R_g}{(R_1' - R) + R_g}\right]^2$$

It is apparent that gain is infinite when $G = G_1' + G_g$, which is a smaller value of negative conductance than required for oscillation in the transmission-type amplifier. Imposing the large gain condition $G \approx G_1' + G_g$, (33) may be rewritten

$$g^2 \approx \frac{4G_g^{\,2}}{(G_g+G_1'-G)^2} \tag{34}$$

Equation (34) bears considerable resemblance to (30), and we will do well to compare the two types of amplifiers which they represent.

For the purposes of comparison, let us neglect the losses represented by G_1', as they are small compared to G_g in any well-designed amplifier. Define the quantity G_{T1} to represent the total positive conductance presented to the current I_1. In the case of the reflection-type amplifier, then, we see that $G_{T1} = G_g$ for optimum loading, and the gain becomes

$$g^2 = \frac{4G_{T1}^{\,2}}{(G_{T1}-G)^2} \tag{35}$$

However, for the transmission-type amplifier, $G_{T1} = G_L + G_g$. Optimum loading will occur when $G_L = G_g = \frac{1}{2}G_{T1}$, and thus the gain at resonance is:

$$g^2 = \frac{G_{T1}^{\,2}}{(G_{T1}-G)^2} \tag{36}$$

A comparison of (35) and (36) will show that the reflection-type amplifier has four times the power gain of the transmission-type for a given set of circuit parameters. This is equivalent to doubling the voltage gain-bandwidth product, merely by the addition of a circulator. In addition, the amplifier stability is improved, because the device always sees a match when looking into the circulator. While this removes none of the stability problems associated with -G, it allows considerable variances in R_g and R_L without causing instability.

It should be noted that the circulator is not an unmixed blessing, especially in very weak-signal applications, as its insertion loss occurs prior to any amplification, and thus degrades the noise figure of the device. This problem can be minimized by refrigerating the circulator, as done in the TELSTAR ground station equipment[9]. In addition, imperfect isolation between ports may support a feedback loop, resulting in oscillation; this is the primary reason for the matched termination shown in Figure 6.

5. Bandwidth

The functional variation of gain with frequency in the parametric amplifier can lead to exceedingly complex calculations. For this reason, we will analyze the device assuming that FL_1 and FL_2 are removed, and that the Q of the tank circuits is sufficient to dispose of the unwanted frequencies. This amounts to changing to an assumption of short-circuited harmonics, but as pointed out earlier, this is of no particular importance. What is important is that the single-tuned circuit case has considerable practical significance, and is not just an approximation chosen for ease of calculation.

Figure 7 shows the equivalent circuit of the transmission-type amplifier when the signal is not at the resonant frequency of the tank circuit. We can analyze the

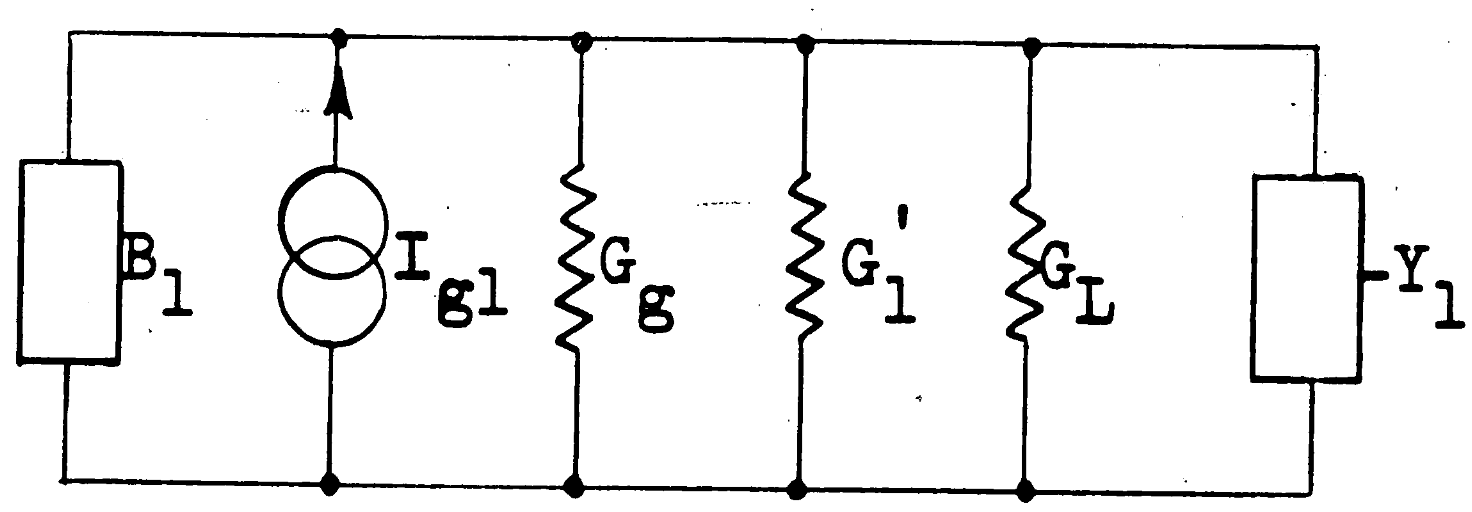

Figure 7. Off-resonance equivalent circuit of parametric amplifier.

single-tuned circuits using well-developed circuit theory techniques. Define the following quantities:

Q_1 = loaded Q of signal tank circuit

Q_2 = loaded Q of idler tank circuit

$$\omega_1 = \Omega_1 + \Delta\omega \tag{37}$$

$$\delta_1 = \Delta\omega/\Omega_1 \tag{38}$$

From the relationship of the signal and idler frequencies (see Figure 3), and the knowledge that the pump frequency is constant, it follows that a positive increment in ω_1 must yield a negative increment, of the same magnitude, in ω_2. Therefore

$$\delta_2 = -\Delta\omega/\Omega_2 \tag{39}$$

The ratio of (39) and (38) leads to

$$\delta_2 = -\delta_1 \frac{\Omega_1}{\Omega_2} \tag{40}$$

With the present definition of δ, the admittance of any single tuned circuit can be described[10] by the relation

$$Y = G[1 + j2\delta Q] \tag{41}$$

where G is the loading of tuned circuit. We may thus write Y_2 directly, and then use (40).

$$Y_2 = G_2\left[1 + j2\delta_2 Q_2\right]$$
$$= G_2\left[1 - j2\delta_1 Q_2(\Omega_1/\Omega_2)\right] \tag{42}$$

Substituting (42) into (28) gives the general expression for Y_1.

$$Y_1 = -\frac{\omega_1\omega_2 C_3^2}{4G_2\left[1 + j2\delta_1 Q_2(\Omega_1/\Omega_2)\right]} \tag{43}$$

Realizing that the off-resonance operation will have an effect on the signal-circuit impedance as well, we may substitute appropriately into (30), making use of (29) and the concept of G_{T1}, developed earlier. This yields the generalized power gain equation, in terms of the bandwidth of the tuned circuits.

$$g^2 = \frac{4G_g G_L}{\left\{G_{T1}\left[1+j2\delta_1 Q_1\right] - \frac{G}{1+j2\delta_1 Q_2(\Omega_1/\Omega_2)}\right\}^2}$$
$$= \frac{4G_g G_L}{\left\{G_{T1} - \frac{G}{1+\left[2\delta_1 Q_2(\Omega_1/\Omega_2)\right]^2}\right\}^2 + 4\delta_1^2\left\{G_{T1}Q_1 + \frac{G(\Omega_1/\Omega_2)Q_2}{1+\left[2\delta_1 Q_2(\Omega_1/\Omega_2)\right]^2}\right\}^2} \tag{44}$$

Defining bandwidth in the customary way -- distance between 3 db. points -- we set (44) equal to one-half the resonance gain as given by (30).

$$G_{T1}\left\{1 - \frac{G/G_{T1}}{1+\left[2\delta_1 Q_2(\Omega_1/\Omega_2)\right]^2}\right\}^2 + 4\delta_1^2 Q_1^2 G_{T1}\left\{1 + \frac{(G/G_{t1})(\Omega_1 Q_2/\Omega_2 Q_1)}{1+\left[2\delta_1 Q_2(\Omega_1/\Omega_2)\right]^2}\right\}^2$$
$$= 2(G_{T1} - G)^2 \tag{45}$$

Equation (45) is rather cumbersome, so we define three new quantities

$$a = \frac{G}{G_{T1}} \tag{46a}$$

$$s = \left[2\delta_1 Q_2 \frac{\Omega_1}{\Omega_2} \right]^2 \tag{46b}$$

$$c = \frac{\Omega_2 Q_1}{\Omega_1 Q_2} \tag{46c}$$

Using Equations (46), we can now rewrite (45)

$$\left[1 - \frac{a}{1+s}\right]^{-2} + \frac{s}{c^2}\left[1 + \frac{a}{c(1+s)}\right]^2 - 2(1-a)^2 = 0 \tag{47}$$

After algebraic calculation, it can be shown that (47) may be expressed in quadratic form:

$$c^2 s^2 + s\left[c^2 + 2ac + 1 - 2(1-a)^2\right] = 0 \tag{48}$$

Blackwell and Kotzebue have shown[6] the approximate solution of Equation (48) to be the form

$$s \approx \frac{(1-a)^2}{(a+c)^2 + (1-a)(3a-1)} \tag{49}$$

under the condition that

$$\left[c^2 + 2ac + 1 - 2(1-a)^2\right]^2 \gg 4c^2(1-a)^2,$$

which is true for large gain and $Q_1 > Q_2$, which generally obtains.

The above method of solution is preferred by this writer because it does not involve any direct assumptions as to the relative magnitudes of Q_1 and Q_2. It also yields a convenient form of the final equation. Any solution to such a complex equation must necessarily be limited, but it is believed that the above procedure is one of the least restrictive available.

If the value of s given by (46b) is substituted into (49), the solution is given in terms of 2δ, the fractional frequency shift. Multiplying this result by (30) will give a gain-bandwidth product in terms of power gain and the square of the normalized frequency deviation:

$$g^2b^2 = \frac{(4G_gG_L/G_{T1}^2)(\omega_2/\omega_1Q_2)^2}{(a + \frac{\omega_2Q_1}{\omega_1Q_2})^2 + (1-a)(3a-1)} \tag{50}$$

where $b = 2\delta$. It has already been shown that for high gain, $G \approx G_{T1}$, therefore $a \approx 1$. Under this approximation the gain-bandwidth product becomes:

$$g^2b^2 = \frac{4G_gG_L/G_{T1}^2}{\left[Q_1 + \frac{\omega_1}{\omega_2}Q_2\right]^2} \tag{51}$$

for the transmission-type amplifier.

By a comparison of Equations (34) and (30), it is readily seen that for the reflection-type amplifier

$$g^2b^2 = \frac{4G_g^2/G_{T1}^2}{\left[Q_1 + \frac{\omega_1}{\omega_2}Q_2\right]^2} \tag{52}$$

Assuming optimum power matching, it is seen that the numerator of (51) becomes unity, while that of (52) becomes four. This confirms the wider bandwidth of the reflection-type device, as predicted earlier.

The above equations show that the parametric amplifier is basically a narrow-band device. In practice, it is difficult to exceed a few percent of the signal frequency in bandwidth for significant gain. Herein is perhaps the parametric amplifier's most serious drawback, although bandwidth may be improved by using considerably more complex circuitry. The device as we have discussed it is quite suitable for point-to-point communications work, especially if ω_1 is high.

It is readily seen from (51) and (52) that in order to maximize the gain-bandwidth product, it is necessary to make ω_2 much larger than ω_1 and/or decrease Q_2. The latter approach is often tried, but if done purely by means of resistive loading, it can have an undesirable effect on the noise figure, as will be demonstrated.

6. Noise Figure

Since the primary reason for using a parametric amplifier is to obtain a low noise figure, it is important to be able to predict the performance of a given circuit in this regard. It is, however, virtually impossible to describe in standard terms the noise figure of a network having negative input and output admittances. For this reason, and because it is often not practical for reasons of stability, we shall not attempt to define a noise figure for the transmission-type amplifier. By virtue of the circulator, however, the reflection-type amplifier exhibits positive input and output admittances, and its noise performance can be accurately predicted by the use of conventional methods. This is fortunate, because the reflection-type amplifier is by far the most widely used.

There are several possible sources of noise in the parametric amplifier:

1. Thermal noise attributable to the diode spreading resistance, R_s.

2. Thermal noise generated in the real conductances in the ω_1 circuitry.

3. Thermal noise generated in the real conductances in the ω_2 circuitry.

4. Shot noise due to the reverse DC saturation current flowing in the diode.

5. Noise due to fluctuations in the value of R_s with pumping[11]. (This is possible because R_s is a weak function of bias voltage, and will vary slightly as the bias is changed.)

Of the above possible sources of noise, it is generally true that only the first three are of significant importance[7,12] provided the diode is not driven into the forward current or reverse breakdown regions. If the diode draws current, the shot noise term becomes very significant, but the amplifier gain generally suffers simultaneously, due to the increased value of the equivalent conductance shunting the capacitor[12].

The calculation of the exact noise figure for the parametric amplifier is a very detailed procedure, much beyond the scope of this paper. There are many excellent solutions of this problem in the literature. We shall utilize the work of Uenohara and Kurokawa[5,7,12] in this area, under the assumptions of large gain and $\omega_1 = \Omega_1$. This will yield the final piece of information essential for the intelligent design of the parametric device.

For the calculation of noise generated within the amplifier, it is convenient to use the equivalent circuit of Figure 5, where G_2 is divided into two separate components, G_{22} and G_{L2}. These parallel conductances represent, respectively, the internal losses of the idler tank and the external idler loading. It is immediately obvious from Figure 5 that the mean square noise currents at ω_1 and ω_2 are, respectively[11]:

$$\overline{i_{n1}^2} = 4kB(T_g G_g + T_1 G_1 + T_d/Q^2 R_s) \qquad (53a)$$

$$\overline{i_{n2}^2} = 4kB(T_2 G_2 + T_i G_{L2} + T_d/Q^2 R_s) \qquad (53b)$$

where k = Boltzmann's Constant

B = bandwidth for noise

T_j = temperature of the conductance having subscript j (in degrees Kelvin)

T_d = diode temperature

The noise current i_{n1} is amplified as if it were a desired signal, and thus the available noise output power is the product of the available noise input power and the amplifier current gain, being

$$N_{01} = \frac{\overline{i_{n1}^2}\, g_{11}^2}{4G_g}$$

$$= \frac{kBg_{11}^2}{G_g}\left(T_g G_g + T_1 G_1 + \frac{T_d}{Q_o^2 R_s}\right) \tag{54}$$

where g_{11}^2 is the power gain for a signal injected and extracted at ω_1. It should be immediately apparent that the value of g_{11}^2 is precisely that of g^2 as given by Equation (34).

Because the parametric amplifier is not a unilateral device, the noise generated in the idler circuitry will also appear at the signal output by the process of parametric mixing. For the reflection-type amplifier, we have assumed that $G_g = G_L$, and thus the available noise power output at ω_1 due to thermal sources at ω_2 is obviously

$$N_{o2} = \frac{\overline{i_{n2}^2}\, g_{21}^2}{4G_g}$$

$$= \frac{kBg_{21}^2}{G_g}(T_2 G_{22} + T_i G_{L2} + T_d/Q_o^2 R_s) \tag{55}$$

where g_{21}^2 is the conversion power gain for a signal introduced at ω_2 and removed at ω_1. It follows that the total available noise output power is given by the sum of (54) and (55).

Friis[13] has shown that the noise figure of an amplifier is specified completely by the ratio of its input and output signal-to-noise ratios. It is apparent that the ratio of output signal power to input signal power at ω_1

is g^2, thus

$$F = \frac{(S_i/N_i)}{(S_o/N_o)} = \frac{S_i}{S_o} \cdot \frac{N_o}{N_i} = \frac{N_o}{g^2 k T_o B} \tag{56}$$

where S_i = available input signal power

S_o = available output signal power

N_i = available input noise power

N_o = available output noise power

T_o = 290°K., standard noise temperature

Substituting in (56) for N_o, under the assumption that $T_g = T_o$, we obtain the noise figure of the reflection-type amplifier.

$$F = \left(1 + \frac{T_1}{T_o}\frac{G_i}{G_g} + \frac{T_d}{T_o} \cdot \frac{1}{Q_o^2 R_s G_g}\right) + \frac{g_{21}^2}{g_{11}^2} \cdot \frac{1}{T_o}\left(\frac{T_2 G_{22}}{G_g} + \frac{T_i G_{L2}}{G_g} + \frac{T_d}{Q_o^2 R_s G_g}\right) \tag{57}$$

For the case where $Q_o \gg 1$, Uenohara has shown that[7]

$$\frac{g_{21}^2}{g_{11}^2} = \frac{g_{21}^2}{g^2} \approx \frac{\omega_1}{\omega_2}\frac{G}{G_{L2}} \tag{58}$$

Assuming all amplifier loss at T_o, and further assuming large gain, it can be seen[5] that

$$F \approx 1 + \frac{G_1}{G_g} + \frac{1}{Q_o^2 R_s G_g} + \frac{\omega_1}{\omega_2}\left[1 + \frac{G_{22}}{G_{L2}} + \frac{1}{Q_o^2 R_s G_{L2}}\right] \tag{59}$$

It can be seen directly from (59) that one way to minimize F is to make G_g large compared to G_1. In terms of circuitry, this requires that the input be overcoupled, which is the standard procedure in minimizing the noise figure of ordinary radio receivers.

To further minimize F, it is desirable that G_{L2} be as large as possible, i.e. the idler termination should be of very low resistance (which is why resistive loading is not recommended for increasing the bandwidth). In order to maximize G_{L2}, the idler termination is often refrigerated, sometimes to liquid helium ($4^{o}K$) temperatures. We shall see later that the need for such procedures is strongly dependent upon the choice of idler frequency. If the idler frequency happens to fall in an area of the spectrum that is generally unused (a rare thing indeed), the idler termination can be an antenna aimed at a "cold" section of the sky[14]. Effective idler temperatures of under 100 degrees are possible with this method, but the existence of broadcasting at the idler frequency would make it impractical.

In an effort to minimize thermal noise, some parametric amplifiers are entirely operated at very low temperatures. While this method very definitely reduces thermal noise, it introduces other problems, the major one being that of obtaining a suitable diode. Because of lack of impurity atom ionization below about 80 degrees Kelvin, silicon and germanium diodes are useless at very low temperatures. Diodes made of gallium arsenide, however, are functional down to helium temperature, and thus are recommended for use where the diode temperature is much below 100 degrees. The development of these GaAs diodes has led to the production of some very low noise amplifiers.

From (59) it is obvious that the entire second term can be made insignificant (and thus practically independent of the value of G_{L2}) if $\omega_1 \ll \omega_2$. For this reason, we desire a high-frequency pump source, generally at least three or four times the value of ω_1. It is worth noting that the noise figure does not improve linearly with increasing ω_3; in fact it is a very weak function of pump frequency so long as ω_3 is greater than about four times the signal frequency[6].

It has been shown by at least two independent groups[6,12] that there exists an optimum idler frequency for the parametric amplifier. Kurokawa and Uenohara have shown that this frequency is given by the relation

$$\tilde{Q}_2 = \frac{\omega_1}{\omega_2} \tilde{Q}_1 \tag{60}$$

where $\tilde{Q}_1$ and $\tilde{Q}_2$ are the dynamic quality factors of the diode at ω_1 and ω_2, respectively (not to be confused with Q_1 and Q_2, the tuned circuit quality factors), and are defined by

$$\tilde{Q}_{1,2} \approx \frac{\gamma}{2} Q_o \Big|_{\omega_{1,2}} \tag{61}$$

for γ less than about one-half. γ is defined by

$$\gamma = \frac{|C_3|}{C_o} \tag{62}$$

The existance of such an optimum is of considerable interest. From (59) it is seen that F should decrease if the idler losses become zero, which implies very low temperatures. However if the idler frequency meets or exceeds the optimum value, it can be shown that no improvement in noise figure will be obtained by refrigerating the idler termination[12]. Within the limitations of cost and equipment, this discovery permits an optimized device to be operated completely at room temperature. Where it is not possible to attain the optimum idler frequency, the optimum noise figure can be attained by reducing the idler temperature to zero[6,7,12].

The last remaining conclusion about the noise performance of the parametric amplifier is that the principal factor in determining the noise figure of the device is the quality factor of the diode, as defined by (31)[6,7,12]. This might well have been implied by inspection of (59). Assuming optimized impedances and idler frequency, it is possible to calculate a minimum noise figure for the amplifier determined entirely by $\tilde{Q}_1$ and the diode temperature[12]:

$$F = 1 + \frac{T_d}{T_g}\left[\frac{1}{\tilde{Q}_1^2} + \frac{1}{\tilde{Q}_1}\sqrt{1 + \frac{1}{\tilde{Q}_1^2}}\right] \qquad (63)$$

This result tells us that in order to minimize the noise figure we must have a diode with a high value of $\tilde{Q}_1$, which implies both large Q_o and γ. Note that even if Q_o is very high, a low noise figure will not be achieved if γ is quite small.[12]

7. Summary

We are presently finished with the development of the basic theory of the semiconductor-diode parametric amplifier. The derivations have in places been lengthy, but it is essential to understand the procedures which led to the results obtained, in order to fully comprehend the functioning of the amplifier. It has not been the purpose of this chapter to develop a new approach to the analysis of this device, but rather to unify the results obtained by some of the many researchers in this field. Expecially with respect to noise theory, it has been necessary to use the results of others without proof, as the proofs are beyond the scope of this paper.

Certain conditions have been derived which allow optimum performance to be derived from the parametric amplifier as regards gain, bandwidth, and noise figure, and it is well to list the more important ones here:

1) Currents or voltages at spurious frequencies should not be presented to the diode.

2) For maximum gain, the device should be operated as close to the threshold of oscillation as is consistent with stability.

3) To increase the gain-bandwidth product, as well as improve stability, a circulator should be used in the signal circuit.

4) The idler Q should be minimized without resorting to resistive loading (unless the termination can be maintained at liquid helium temperature or below).

5) The input circuit should be over-coupled to the optimum point.

6) The dynamic quality factor of the diode should be as high as possible.

7) The idler frequency should be optimized, which requires a pump source of both high frequency (compared to ω_1) and excellent frequency and amplitude stability.

Having thus determined the prerequisites for an optimized parametric amplifier, we shall proceed to their application to a practical device.

III. The Practical Parametric Amplifier

I. Configuration

It was decided that the experimental amplifier should be of the reflection-type, in the interests of stability and ease of adjustment. Because of the limitations imposed by existing equipment --largely for S and X bands -- the pump and signal frequencies were chosen to be 12.00 gc. and 3.95 gc., respectively. It is then apparent that the idler frequency is fixed at 8.05 gc., a restriction which almost certainly will prevent any idler optimization to take place.

As with most electronic devices, any configuration that will do the job is satisfactory. From the start, an all-waveguide amplifier was ruled out because of the size disparity of S and X band guide, and its attendant mechanical problems. Considerable thought was given to the "hybrid" amplifier[9], in which the signal and idler circuits are contained in rectangular waveguide, and the pump power is fed in coaxially. In such an amplifier, the diode is simultaneously a part of the coaxial and waveguide structures, and severe mechanical and electrical problems could be foreseen.

The structure finally settled upon is an all-coaxial one suggested by Dr. Nikolai Eberhardt. A cross-sectional view is shown in Figure 8 -- the device has circular symmetry about the vertical axis except for the pump

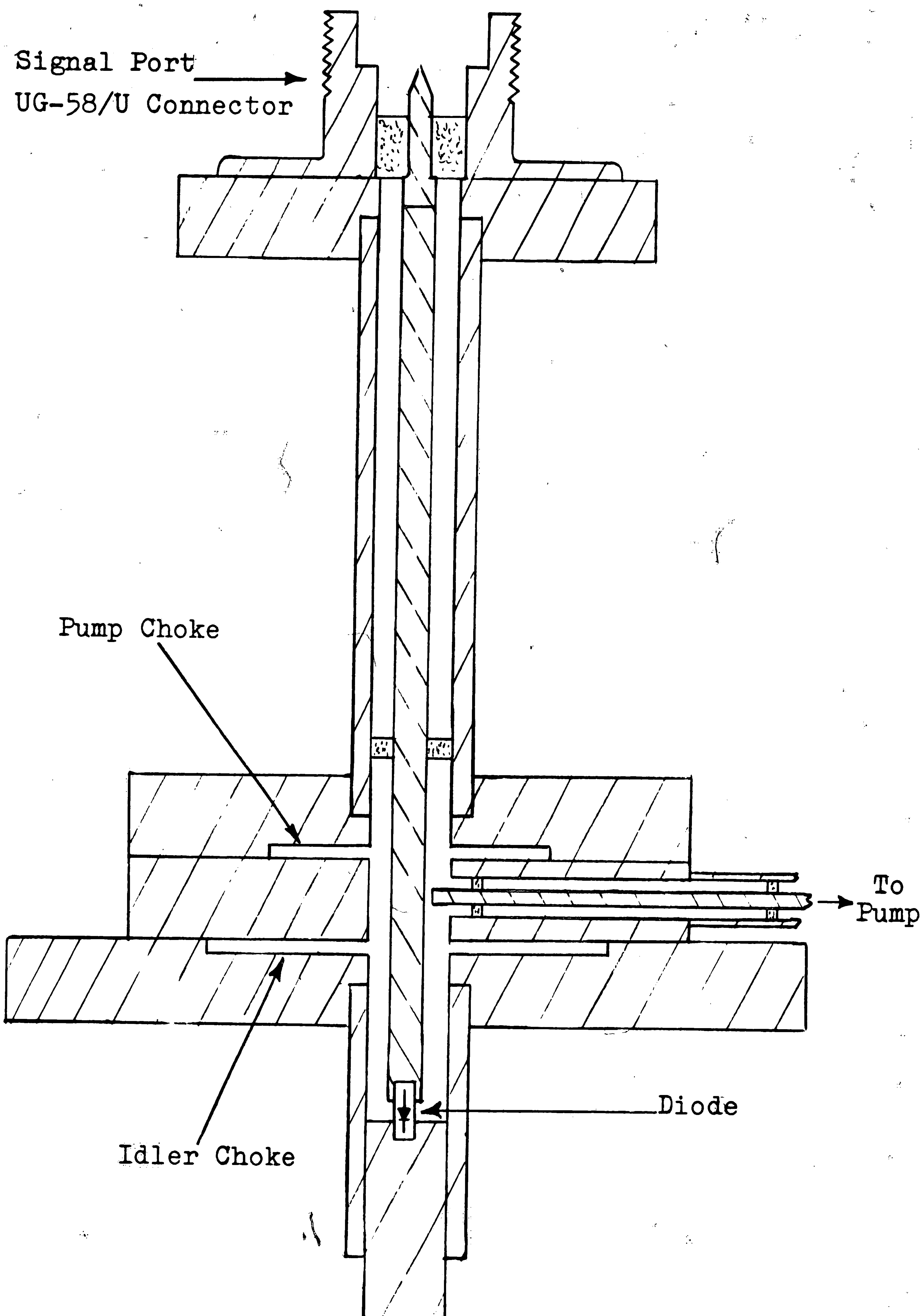

Figure 8. Cross-sectional view of amplifier

coupling line. Mechanically, the amplifier is quite simple, and lends itself easily to modifications because of its "modular" assembly.

Electrically, the proposed theory of operation is quite straightforward. The two radial line sections present infinite series impedances to coaxial wall currents at the pump and idler frequencies. In addition, the diode -- mounted in a shorting plane -- is so spaced from the radial chokes as to form resonant cavities for ω_3 and ω_2. The diode has a low impedance at these frequencies, and thus does not significantly alter the short circuit termination.

The cavity formed by the diode mount and the choke nearest it exhibits quanter-wave resonance at the idler frequency. This short length is chosen to minimize the idler stored energy, and hence the idler Q, in the interests of bandwidth. The next choke forms a resonance with the diode and the loading of the idler choke at the pump frequency, to facilitate the transfer of pump power to the diode. The signal circuit is tuned with external stubs, the signal being fed through the upper fitting in Figure 8 by means of a circulator.

Pump power is coupled into the cavity capacitively, at a pump-voltage antinode.

The diode, being mounted at a low impedance point, is essentially current operated. This is necessary, as the low impedance of the diode to pump frequency precludes mounting at a voltage antinode. As no provision has been made for biasing, it will be necessary to use a biasing tee, as if often done with traveling-wave tubes to bias the helix. Such a device has the equivalent circuit shown in Figure 9, and is inserted directly into

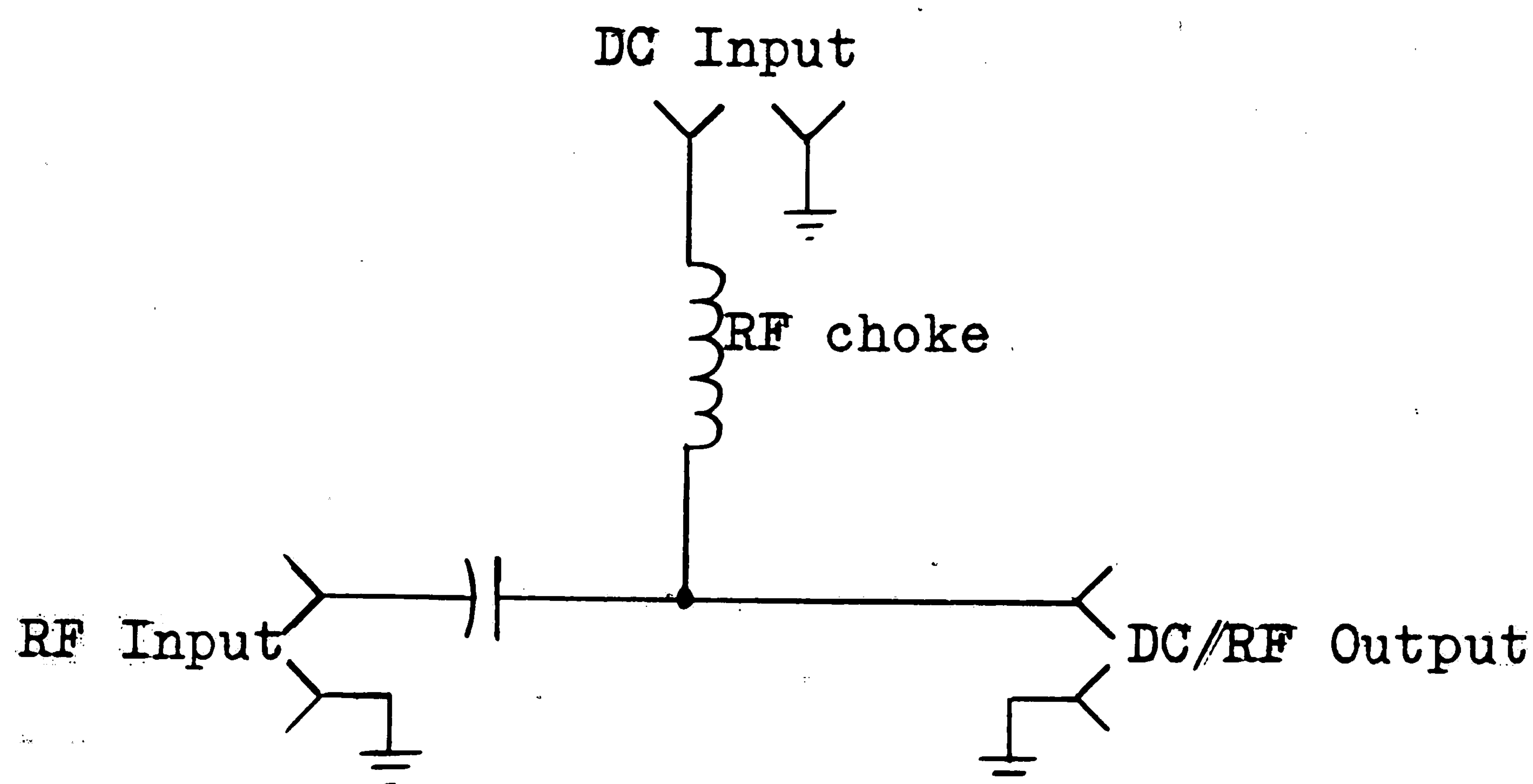

Figure 9. Equivalent circuit biasing tee.

the coaxial signal circuit. The effect on amplifier performance is minimal, provided a unit with low VSWR is used.

As presented, the amplifier is notable for its mechanical and electrical simplicity. It has three features, however, which may lead to later trouble:

1) Because of its mechanical arrangement, tuning is difficult. This could be remedied with a trombone center conductor, but doing so adds contact and mechanical support problems.

2) Due to the low impedance seen by the external

signal circuit, particular care may have to be taken in matching this device to the generator.

3) By the very nature of the cavities, it is possible for odd-order intermodulation products to be presented to the diode. This should not be a serious problem provided the signal level is much below the pump level, as is usually true.

There was a definite reason for choosing the signal frequency such that none of ω_1, ω_2, or ω_3 is harmonically related; that being that it is possible to couple considerable noise into the circuit from the pump by means of subharmonics if the three frequencies are harmonically related. This is not an unnecessary precaution, for there is considerable noise in the pump circuit generated by the reflex klystron used as a source. An incidental benefit of such a frequency choice is that there is never any doubt as to whether it is, for example, the idler frequency or the second harmonic of the signal frequency that is being measured.

2. The Diode

The diode used in this amplifier is one of a series of Western Electric microwave diodes kindly supplied by that organization. It has a cutoff frequency of 160 gc., zero bias capacitance of 0.604 pf., and a reverse breakdown (10 μa.) of 19 volts. Little else is known about the diode, but not much other information is actually required.

From our knowledge of cutoff frequency, the static Q is readily determined:

$$Q_o = \frac{\omega_c}{\omega_1} \quad 40 \ .$$

Similarly, the value of R_s can be found from the definition of ω_c:

$$R_s = \frac{1}{\omega_c C_o} \qquad 1.65 \text{ ohms.}$$

From the above results, this appears to be a very good diode.

It is necessary to know the approximate capacitance variation in advance, both to allow the approximate cavity loading to be evaluated, and to permit a rough evaluation of $\widetilde{Q}_1$. We do not know anything in detail about the diode structure or doping, but we can fairly safely assume this junction to be of the diffused type[16], which yields a capacitance variation of the form

$$C(V) = \frac{C}{\sqrt[3]{1 - \frac{V}{V_o}}} \ ,$$

where V_o is the junction contact potential. This also is unknown, but for reasonably doped junction diodes, it is safe to assume a value of about 0.7 volts[16]. With this assumption for V_o, we can plot the capacitance of the junction as a function of voltage (Figure 10). Although this curve is not exact, it is a very good approximation, even for other values of V_o. The diode capacitance could, of course, be measured, but the mathematical approximation is likely to be more accurate due to the fact that stray capacitances in measuring are likely to be of the same order of magnitude as the diode capacitance, unless a very accurate high frequency bridge is used.

From Figure 9, we see that the total capacitance variation from slight forward bias to reverse breakdown bias is such as to make γ very large, perhaps even greater than unity. It is, therefore, a reasonable assumption that γ will at least equal 0.5, and in that case we see that

$$\tilde{Q}_1 = \tfrac{1}{4}Q_o \approx 10 .$$

It thus appears that this diode will be suitable for use in the parametric amplifier.

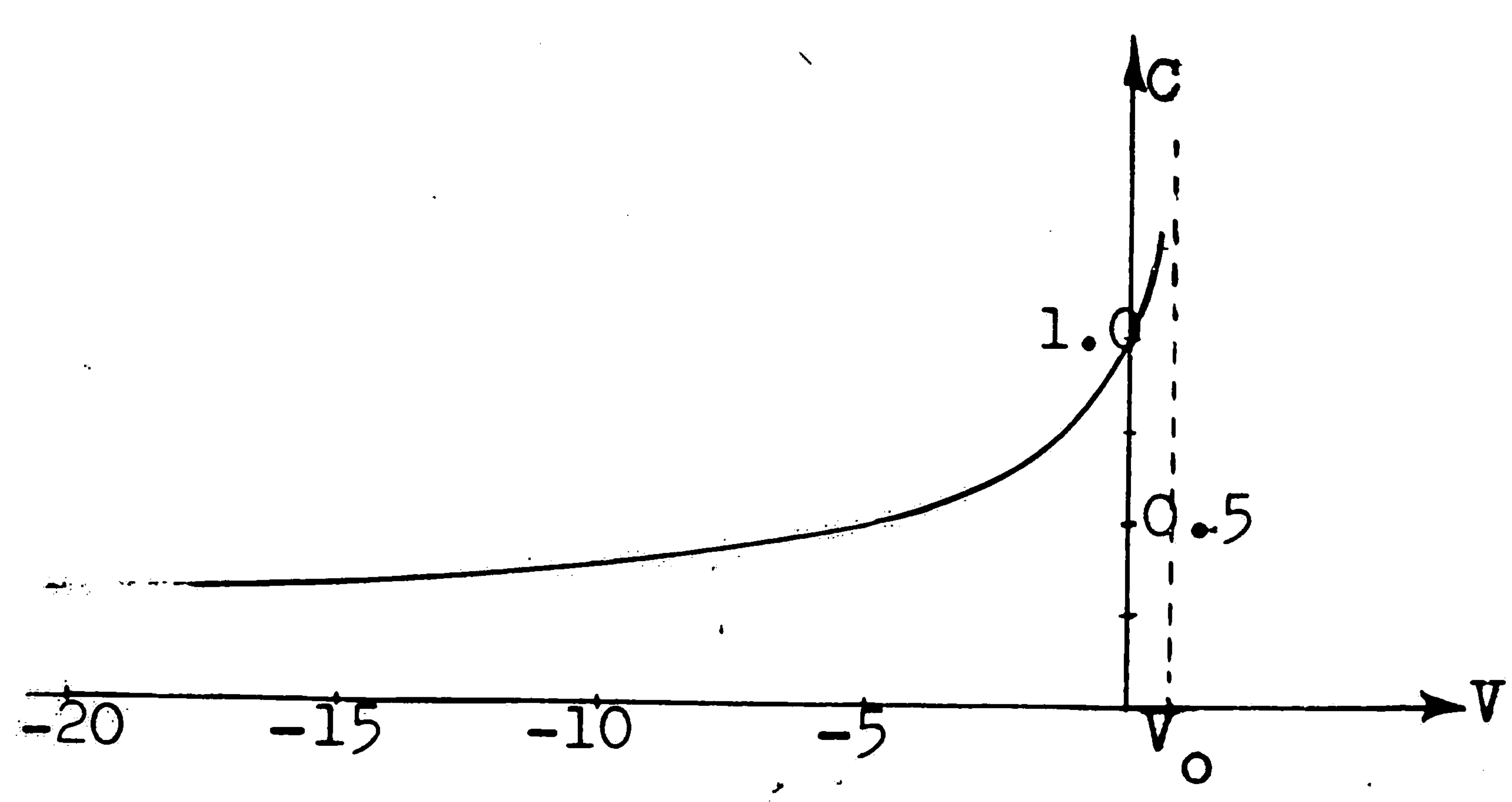

Figure 10. Normalized capacitance variation of a diffused junction.

3. Constructional Details

Although most of the amplifier construction is straightforward, there are a few things worthy of special note.

The dimensions of the coaxial line that forms the heart of the amplifier were chosen to give a nominal 50 ohm line impedance, at the same time presenting a minimum mechanical discontinuity to type N coaxial connectors. The type N connectors were selected because of their constant impedance and low VSWR characteristics at the signal frequency. It being desirable to use as many standard sizes of tubing as possible, the dimensions were finally chosen to be .250 inches for the inner diameter of the sleeve and .110 inches diameter for the inner conductor diameter. (The latter is standard #35 brass drill rod). Both these sizes are found from the familiar equation for air dielectric coaxial line

$$Z_o = 60 \ln \frac{d_{outer}}{d_{inner}} .$$

Note that because the coaxial line in the amplifier is air dielectric, the line and free space wavelengths are identical, given by

$$\lambda = \frac{300}{f} \qquad (64)$$

where λ is wavelength in meters, and f is frequency in megacycles.

The radial chokes used for the pump and idler frequencies present some practical design problems, because their impedance varies as a complex function of Bessel Functions. For this reason, they may not simply be chosen as a quarter-wavelength long at the desired resonance frequency. From basic field considerations, it is possible to show that for a radial line whose load impedance is zero[15]:

$$Z_i = jZ_{oi} \frac{\sin(\theta_i - \theta_L)}{\cos(\psi_i - \theta_L)} \qquad (65)$$

where

$$\theta(kr) = \tan^{-1}\left[\frac{N_o(kr)}{J_o(kr)}\right]$$

$$(kr) = \tan^{-1}\left[\frac{J_1(kr)}{-N_1(kr)}\right]$$

$$Z_o(kr) = \eta \sqrt{\frac{J_o^2(kr) + N_o^2(kr)}{J_1^2(kr) + N_1^2(kr)}}$$

$$k = \omega\sqrt{\mu\epsilon} = \omega/c \text{ for air dielectric}$$

where the quantities are

Z_i = input impedance of radial line

r = radius of line, measured from center of inner conductor of coax. (See Figure 11)

J = Bessel function of the first kind

N = Bessel function of the second kind

c = velocity of light

η = 377 ohms for air or vacuum.

The subscripts i and L denote a quantity evaluated at r_i or r_L respectively.

It is obvious that (65) will become infinite -- the desired condition for operation as a choke -- when

$$\psi(kr_i) - \theta(kr_L) = \pm \frac{\pi}{2} \qquad (66)$$

It can be shown that only the negative sign on the right hand term yields a valid solution, thus

$$\theta_L = \Psi_i + 90^\circ \tag{67}$$

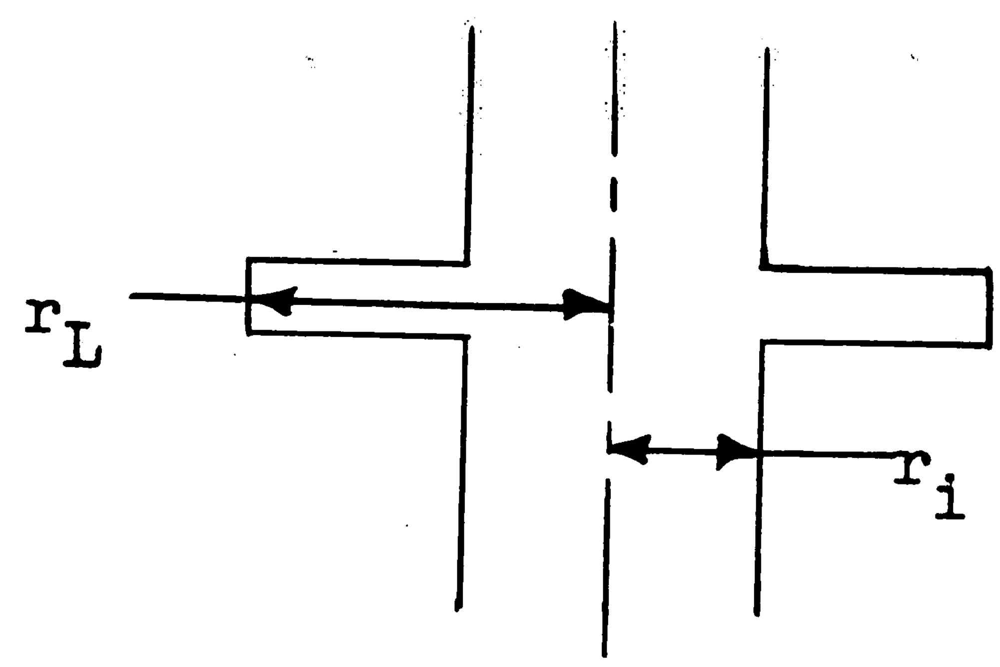

Figure 11. Method of measuring r for radial line calculations.

Having established the above condition, the determination of the choke length is reduced to a matter of calculation, which we record in a stepwise fashion:

a) Evaluate k and Ψ_i from Equations (65), utilizing tables of Bessel functions[16,17].

b) Determine θ_L from Equation (67).

c) Substitute the value obtained for θ_L in the definition of θ_L, which will yield an equation of the form

$$(\tan \theta_L) J_o(kr_L) = N_o(kr_i) \tag{68}$$

Equation (68) must be solved graphically, by choosing values for kr_L, determining the associated Bessel functions, and plotting.

The application of the above procedure yields for the choke lengths

$$(r_L - r_i)_{pump} = 0.820 \text{ cm.}$$

$$(r_L - r_i)_{idler} = 1.229 \text{ cm.}$$

Equation (65) gives the input impedance of the choke at any frequency, provided k is evaluated for the desired value of ω. The impedance of the chokes and the diode constitutes virtually all of the reactive cavity loading. Using a Smith Chart, these impedances are readily transferred to a single plane, and the cavity lengths may be directly calculated with the known loading.

4. Pump Power Source

As mentioned previously, the primary reason for the choice of the pump frequency was the availability of X-band waveguide and equipment. It is obvious from Figure 8, however, that the pump signal is fed in coaxially; the coupling being just outside the end of the idler cavity. This manner of injection requires a waveguide-to-coaxial adapter, which was built in the usual manner, as shown in Figure 12. The adapter used has a measured insertion loss of 3.3 db.

It is interesting that this type of pump injection eliminates the need for a filter in the pump circuit to reject the signal and idler frequencies. This is so in the case of the idler because the pump injection is outside the idler cavity, and only very small fringing fields of ω_2 exist at the injection port. Likewise, signal energy cannot flow out of the amplifier by way of

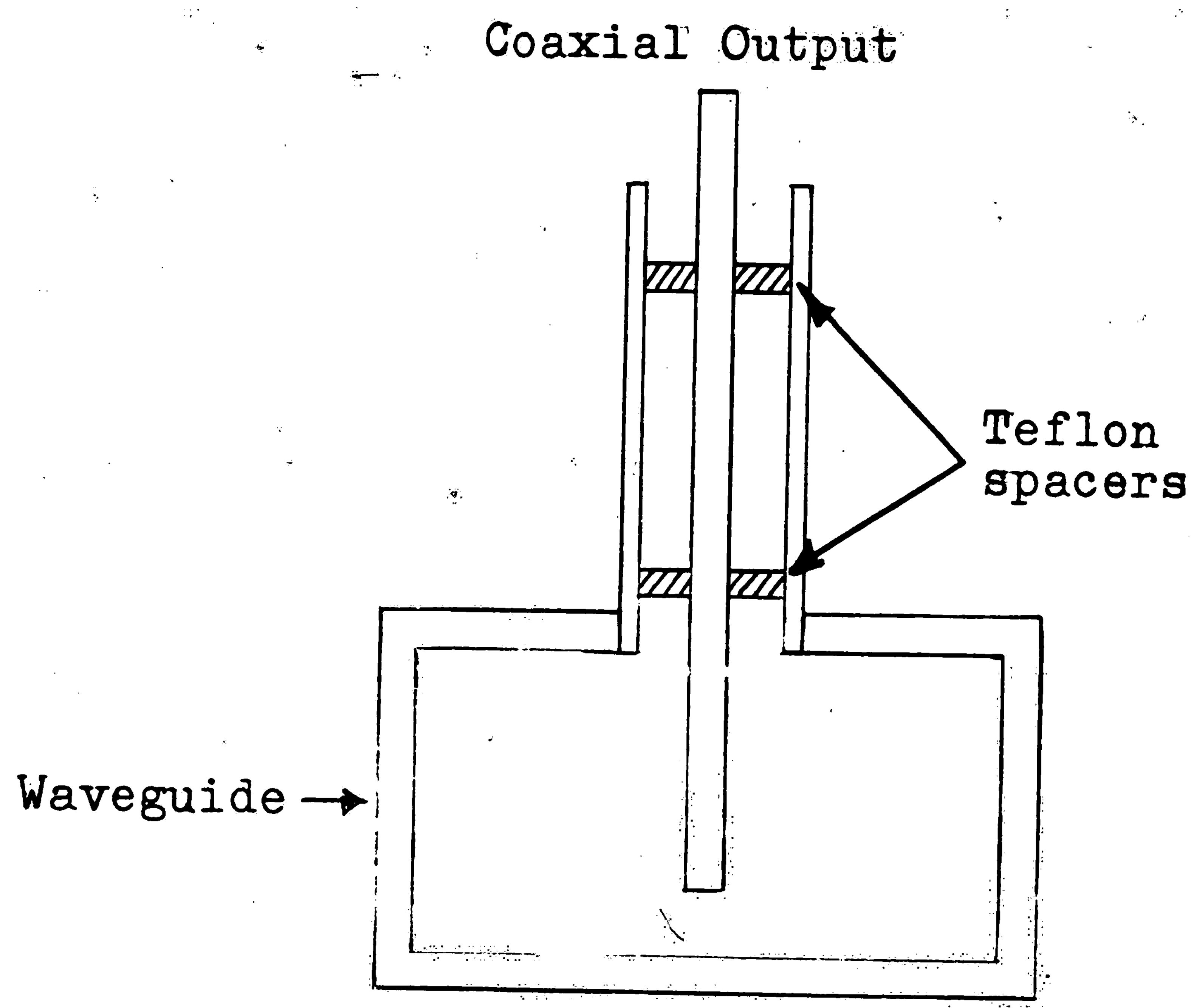

Figure 12. Cross-sectional view of pump coupling adapter.

the pump because signals at ω_1 are well below the cutoff of X-band waveguide.

A diagram of the pump source is shown in Figure 13. A Varian X-13 reflex klystron is used as it has been found to demonstrate excellent frequency stability and rapid thermal stabilization. It is capable of delivering about 90 milliwatts to a matched load at 12 gc., but because of the coaxial adapter losses, the available pump power is on the order of 42 mw.

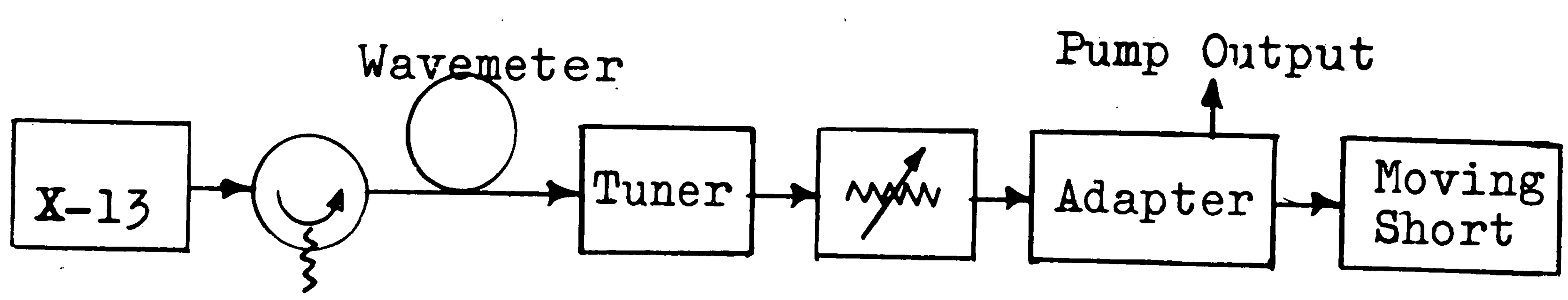

Figure 13. Pump frequency source.

5. Signal Source and Detection

Several possibilities exist in the laboratory for the generation of a signal at 3.95 gc. They are:

a) Alfred Electronics Microwave Sweep Oscillator with S-band head. (This device also has a power leveler and X-band head as accessories).

b) Western Electric 431A reflex klystron powered by regulated supply.

c) U.S. Army Signal Corps model P412-LAG 1 signal generator, which has a maximum output of about 40,000 microvolts.

Any or all of these devices are available and may be used, depending on suitability. It is anticipated that the sweep oscillator will be most useful in bandwidth determinations.

After amplification, the output signal will be detected by either an AN/APR-4 radar receiver, or a Hewlett-Packard 431 Power Meter. The former method is of use if the signal is of a very low level. The receiver is also desirable because of its narrow bandwidth, compared to a thermistor detector.

6. Summary

In this chapter, we have introduced the structure and theory of the amplifier to be evaluated, and noted the design procedure which was utilized. The parametric diode has been chosen and roughly evaluated. We have also undertaken a description of the equipment used to produce the signals at ω_1 and ω_3.

Having thus seen the proposed amplifier, we shall proceed to its experimental evaluation, where the design assumptions will be either verified or disproven.

IV. Experimental Techniques and Results

1. Initial Adjustments

Before anything can be attempted with the amplifier, it is necessary that the cavities be adjusted to the proper resonant frequency. This must be done with the diode biased, as the cavity frequency will obviously be changed if the reactance of the diode changes. The bias may be introduced through biasing tee, as shown in Figure 9, and the cavity resonance may be detected by injecting pump frequency power into the signal input and measuring the ratio of forward to reflected power. As the chokes are not perfect, some power will couple into the cavity, and a decrease in reflected power is to be expected at the resonant frequency of the cavity.

Using point-by-point methods, the above procedure would be most time consuming; however, with the sweep frequency method of Figure 14, it becomes quite rapid. The signal generator has an X-band head and this is used in conjunction with the power leveler to obtain an essentially flat power output over any range of frequencies -- it is possible to sweep the entire X-band if necessary.

Because of the directional couplers, the DC voltage output of CR_1 and CR_2 is proportional to forward power, while that of CR_3 is proportional to reflected power. The output of CR_1 serves as the sensor for

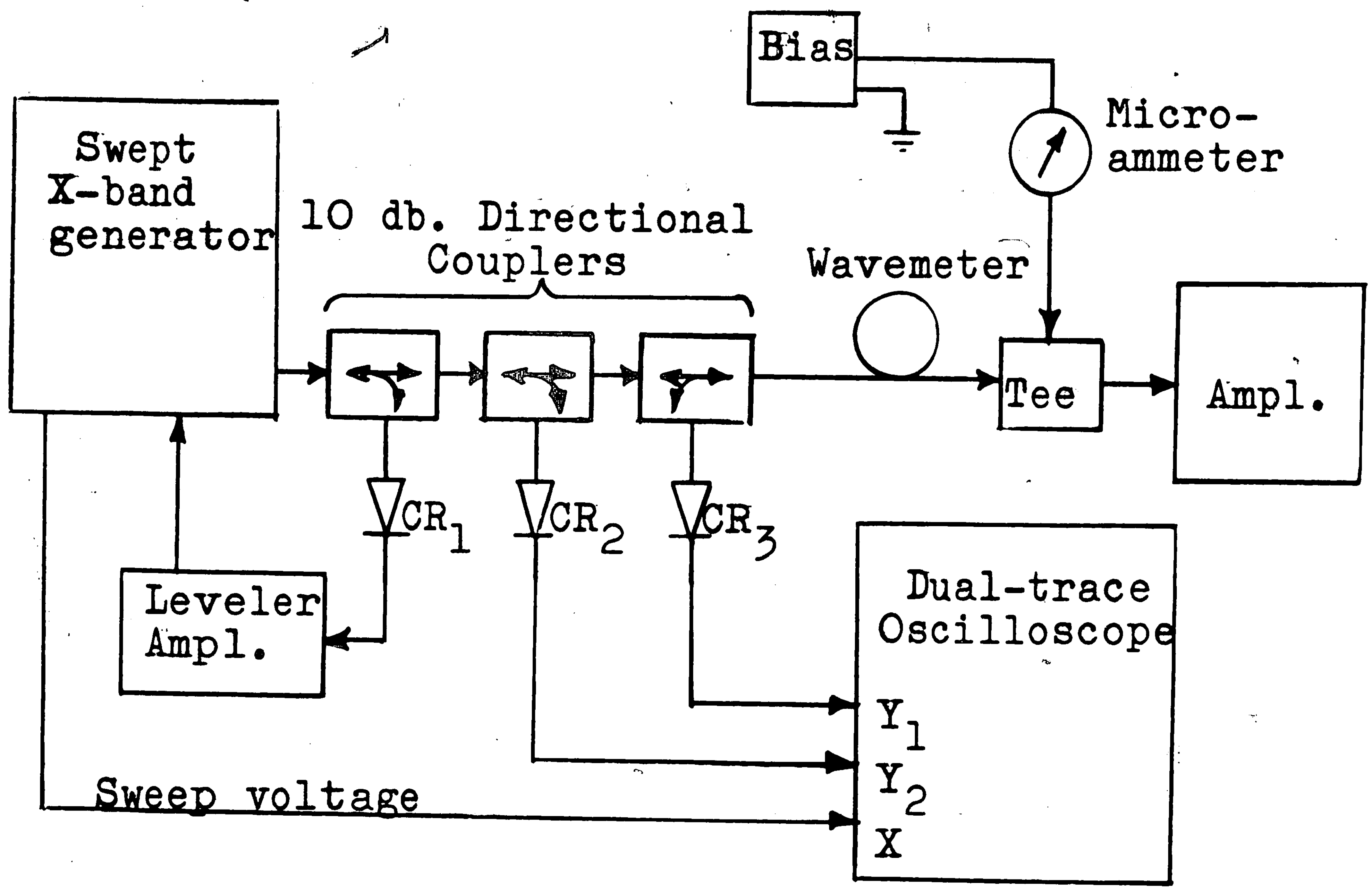

Figure 14. Experimental arrangment for setting cavities to resonance.

forward power, which is amplified and applied to the sweep generator as an error signal to maintain constant power output. The other two outputs are displayed simultaneously on the dual trace oscilloscope. The absorption frequency of the wavemeter is easily seen on the reflected power curve, thus making it a simple matter to locate accurately the resonance of the cavity.

Due to the excellent operation of the leveler, it became necessary to monitor only the reflected power trace. This was closely studied by using a 5 millivolt per centimeter ac coupled oscilloscope plugin. When the X-band was swept, resonances were detected near 8 and 11.9 gc., which can be recognized as the idler and pump resonances, respectively. A third resonance near 11 gc. was found to be caused by an internal absorption in the biasing tee.

By varying the length of the cavity, the pump resonance was adjusted to 12.0 gc. at -10 volts bias.

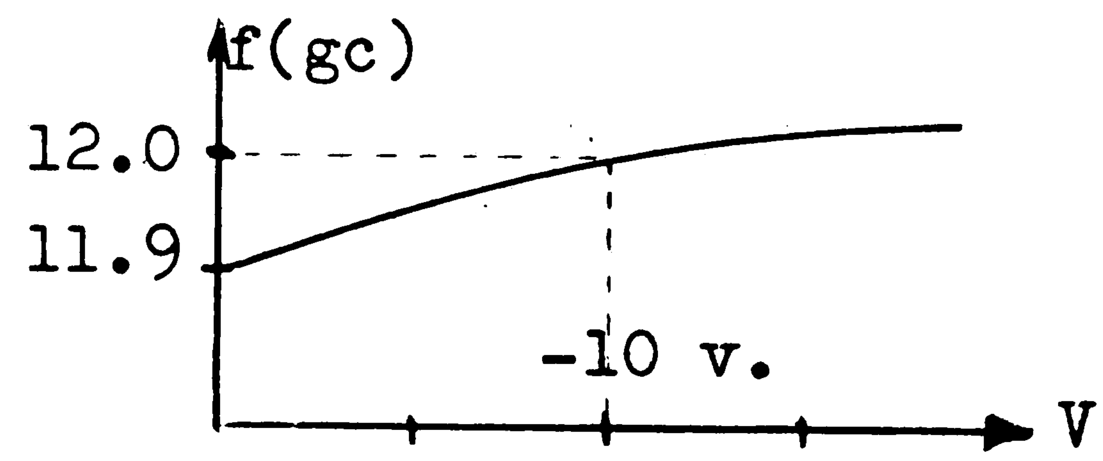

Figure 15. Cavity absorption frequency as a function of diode bias.

The results of Figure 15 are obtained by accurately measuring the frequency of the reflected power minima with the wavemeter and the oscilloscope. This is necessary because the inertia of the recorder pen prevents it from responding accurately to the sharp absorption pattern of the wavemeter.

One disturbing fact was noted when the preceding plots were taken: the 8 gc. resonance appeared very wide and nonuniform, extending over nearly 300 megacycles. While part of this may be due to the VSWR of the biasing tee, at least some of it is definitely caused by the amplifier, as confirmed by varying diode bias. Many possibilities for undesired resonances exist, and these could complicate the amplification picture.

With the cavity resonances adjusted, all is in readiness for the final adjustment of the signal circuits.

2. Passive Measurements

One of the primary problems encountered with the parametric amplifier is the multiplicity of adjustments which must be made in practice in order to optimize the performance of the device. To further complicate matters, many of these adjustments interlock, and the simultaneous optimization of both the signal and pump circuits can easily become a task bordering on the impossible. For this reason, a method of optimizing the amplifier performance by relatively simple means is highly desirable in practical use of the device.

In the field of microwave tubes, the so-called "cold" test is very useful in setting up a device for optimum performance. Kurokawa has recently shown[19] that a similar procedure is usable with the parametric amplifier, allowing the noise figure to be very accurately predicted before the pump is even turned on. The process also gives order of magnitude results for amplifier gain. The cold test is both simpler and more accurate than the trial and error method, and will reveal, in addition, whether or not the diode in use has significant parallel leakage conductance. If this occurs, noise figure optimization is very nearly impossible, and a better diode should be used.

The fact that such cold measurements can be made hinges on the derivation of noise figure which showed that F depends very strongly on $\tilde{Q}_1$. From this we can determine optimum values of R_s/R_g and R_s/R_L, essentially by measuring the impedance locus at the signal port of the parametric amplifier. We will not attempt to derive Kurokawa's mathematical results, but we will show through plausibility arguments how the cold test works.

It can easily be seen by inspection of the equivalent circuit (Figure 5) of the amplifier that its input impedance consists of a constant-valued resistive part, plus a reactive part which varies with the bias applied to the diode, due to the change in diode capacitance with bias. It follows, then, that if a plot were made of the impedance locus of the input as a function of diode bias voltage, the locus would map onto a constant resistance circle of the Smith Chart, assuming proper choice of a reference plane.

What has been said above is true so long as the diode is operated on the constant current section of its reverse characteristics. As the operating point approaches a current-flow condition, either forward or reverse, a significant parallel conductance appears across the terminals of the diode equivalent circuit. As this conductance -- and to some extent, the value of R_s -- varies with bias voltage, the assumption of constant resistance is invalidated, and the mapping will not lie on such a circle in the Smith Chart. A radical departure of the locus from a constant resistance circle for all reference plane choices is indicative of a poor diode, which should be replaced before further work is attempted.

Experimentally, the locus is plotted using an arbitrary reference plane. This circle is then rotated about the center of the Smith Chart until it fits a constant resistance circle. This determines the reference plane, and the point where the locus crosses the real axis of the Chart gives R_s/R_g if the locus is circular. It is desirable that the locus be symmetrical about the real axis, as this implies no net reactance is added to the input circuit by the diode. Kurokawa shows[19] this symmetry to be a necessary (but not sufficient) condition for optimum noise performance.

The diode dynamic quality factor, $\tilde{Q}_1$, can be defined in a form equivalent to Equation (61) in somewhat different terms, which allow its calculation from the impedance locus.

$$\tilde{Q}_1 = \frac{1}{\omega(2K_1)R_s} \qquad \frac{\text{Total reactance variation}}{4R_s}$$

$$= \frac{2\Delta X}{4R_s} \tag{69}$$

where K_1 is defined by the series

$$\frac{1}{C(t)} = \frac{1}{K_o} + \frac{1}{K_1} \cos \omega_3 t + \ldots \quad .$$

ΔX can be found from the impedance locus, it being simply the change in reactance observed from one end of the locus to the other as the bias is varied.

We now have all the information necessary to evaluate the noise performance of the amplifier. In addition, Kurokawa states that for optimum gain, the impedance locus (if it is symmetrical) should cut the straight lines formed on the Smith Chart by connecting the points $(\infty, j\infty)$ and $(0, \pm j2)$.

Kurokawa and Uenohara have shown[12] that the minimum noise condition is given by

$$\frac{R_s}{R_g} = \frac{1}{\tilde{Q}_1\tilde{Q}_2 - 1} \tag{70a}$$

and $$R_s/R_L \rightarrow \infty \tag{70b}$$

Using (69), (70a) may be rewritten

$$\frac{\Delta X}{R_g} = \frac{2\tilde{Q}_1}{\tilde{Q}_1\tilde{Q}_2 - 1} \tag{71}$$

The noise figure may now be determined from the nomograph in Reference (12), or by substituting (69) and (71) into the noise figure equation:

$$F_{min} = 1 + \frac{T_d/T_g}{\tilde{Q}_1\tilde{Q}_2 - 1}\left[1 + \frac{\omega_1}{\omega_2}\tilde{Q}_1\tilde{Q}_2\right] . \tag{72}$$

(Equation (72) is merely a restatement of (63) without the assumption of optimized idler frequency). The substitution yields

$$F = 1 + \frac{R_s}{R_g}\left[1 + \frac{\omega_1}{\omega_2}\left(1 + \frac{R_g}{R_s}\right)\right] , \tag{73}$$

where R_g/R_s is read from the Smith Chart as noted earlier. This result applies strictly only if the locus meets the conditions of (68b), but this condition will generally obtain at large gain.

To measure the locus on our amplifier, the experimental arrangement of Figure 16 was used. The two double-stub tuners were found necessary for easy adjustment of input impedance. One would probably have sufficed, but the adjustment is highly critical.

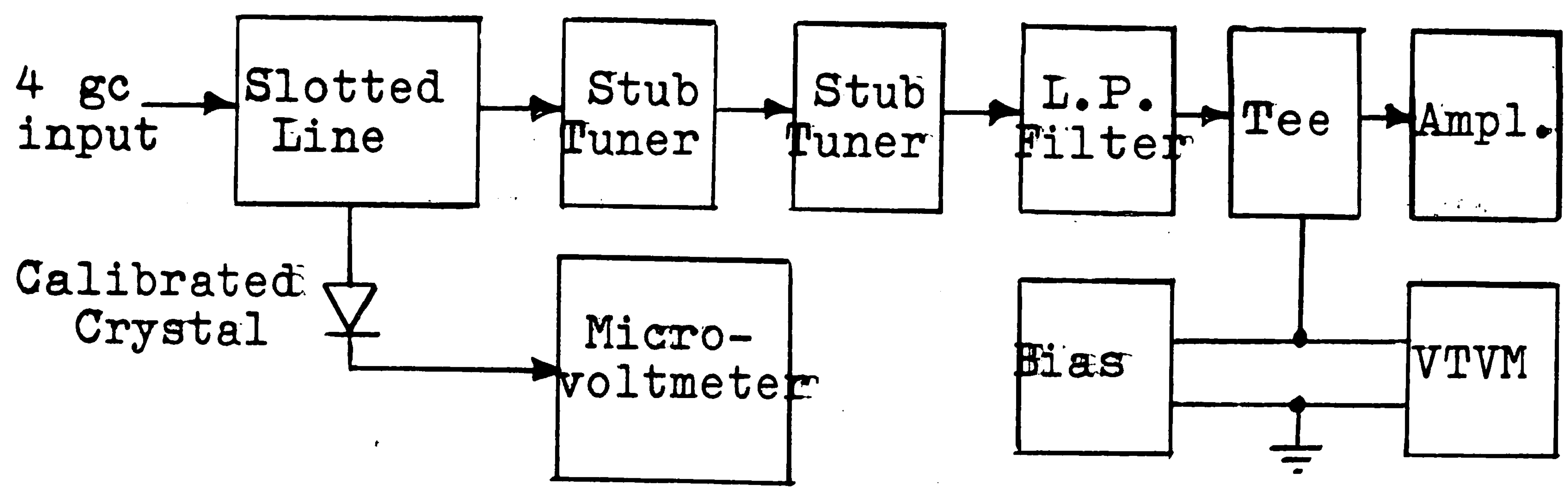

Figure 16. Experimental arrangment to measure impedance locus of parametric amplifier.

The impedance locus of the device is plotted in Figure 17. From this plot, it is seen that

$$\frac{R_s}{R_g} \approx 0.85$$

from which Equation (71) gives the expected noise figure

$$F \approx 4.4 \text{ db.}$$

This is not a particularly good noise figure for a parametric amplifier, but it is quite competitive with electron tube devices at these frequencies. The theoretical minimum of noise figure for the frequencies used can be shown to be about 2.5 db.[6]

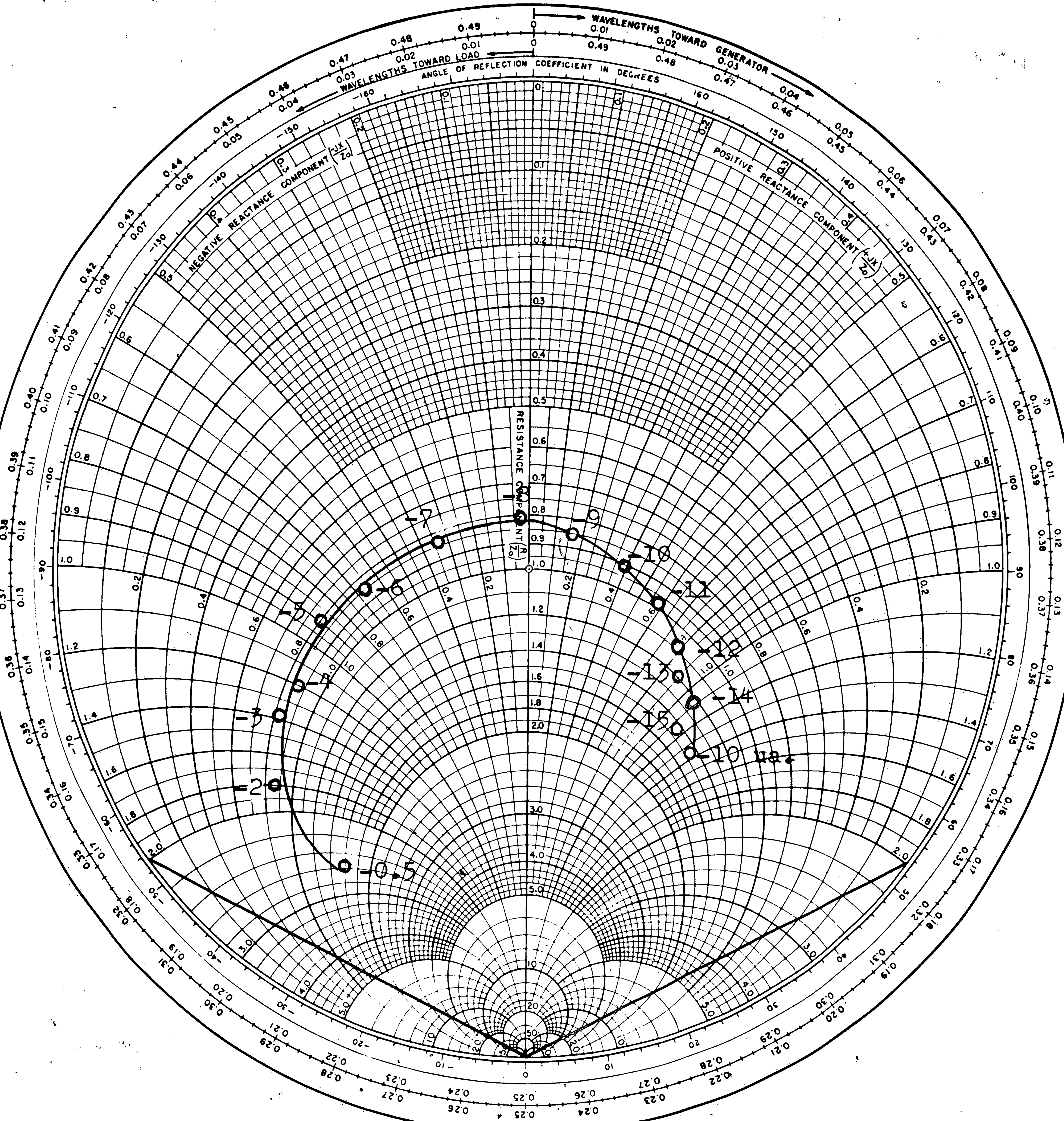

Figure 17. Impedance locus of the amplifier

Part of the locus is seen to depart rather markedly from the 0.85 resistance circle for high reverse bias. It appears this is due to increased current flow through the diode, as mentioned earlier. The noise figure will suffer as a result of this effect, and also due to the net reactance added to the input by the diode, as seen by the asymmetry of the locus.

We shall shortly compare this prediction with our observations.

3. Amplifier Gain

In order to measure the amplifier gain, the configuration of Figure 18 is used.

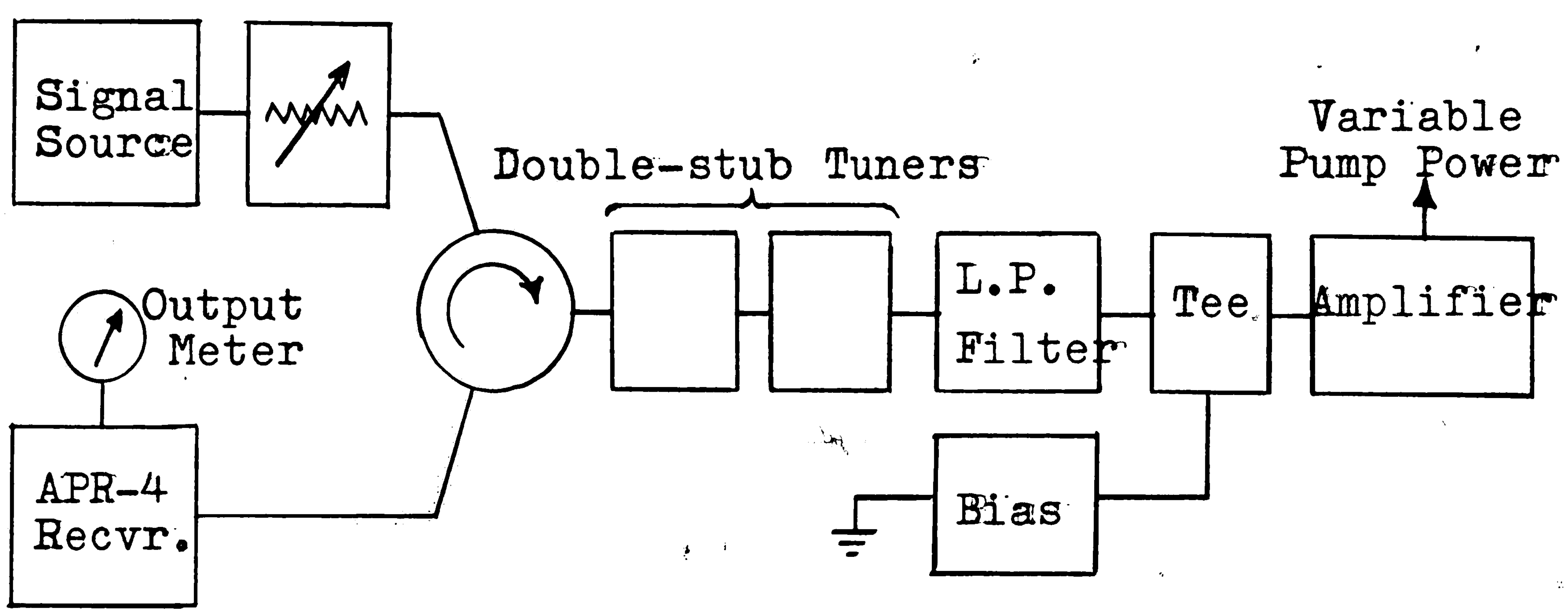

Figure 18. The operating parametric amplifier.

The lack of an S-band wavemeter is a distinct disadvantage here, but this piece of equipment did not arrive as scheduled. In its stead, the dial calibration of the APR-4 receiver is used; this has been checked with a transfer oscillator and found to be accurate within approximately ± 5 megacycles. This accuracy is implied in the later reports of measurements.

With the signal generator turned off, but not disconnected, the loaded amplifier exhibits a very strong oscillation at 3.955 gc. The pump attenuator provides a smooth regeneration control, allowing the threshold to be very closely approached.

Several methods of determining gain were tried, but the broadband methods were inadequate because of the high harmonic output of the signal source. The method used was to adjust the signal level to bring the amplifier output to a convenient reference point on the APR-4 meter; then disconnect the amplifier from the receiver and replace it by the signal generator, readjusting the attenuator to achieve the same reference level. The difference in attenuator settings equals the amplifier gain.

Using this system at 3.955 gc., maximum gain of 4.8 db. was observed with a positive diode bias of 0.18 volts. It was observed that maximum gain occurred with zero or slight positive bias voltages. This is in accordance with the results observed by Uenohara[7], and appears to be due to the large capacitance variation available on the portion of the curve between zero volts and the contact potential.

4. Conclusions and Comments

It will be noted that no data on bandwidth or measured noise figure have been presented. This is due to the fact that the necessary measuring equipment for the determination of these factors has not arrived. This is indeed unfortunate; however, in the matter of noise figure, the predicted value generally is within 0.5 db. of the measured value[19], and thus it seems safe to assume a maximum noise figure of 5 db. for the amplifier.

The bandwidth of this device is, by qualitative observation, very narrow. No equipment capable of measuring frequency accurately in this range is presently available, but from observation of receiver output with varying input frequency, the bandwidth appears to be no more than a few megacycles at maximum gain. (This method is permissible because of the wide bandwidth of the APR-4 receiver).

The basic soundness of the amplifier design has been demonstrated, as evidenced by the observed gain. This was our main objective. It is obvious that further optimization is required, however, and it seems apparent that the primary place for this is in the signal circuit, where an improved method of matching the diode is required. This could take the form of a resonant circuit, capable of providing sufficient overcoupling for the diode to lower the noise figure by moving the impedance locus to a larger constant resistance circle.

In addition, greater gain could be achieved by increasing pump power, which requires that the losses in the waveguide to coaxial adapter be reduced. This could most easily be effected by decreasing the length of the coupling line. If this can be done, no increase in klystron output should be required.

For ease in adjusting the device to resonance, it now seems desirable to add a variable capacitive susceptance between pump and idler chokes in the form of a screw. This would make the initial resonance adjustments easier.

As is readily seen, much more can be done to optimize the performance. Time does not permit a study of these alterations, but it may be stated that the basic amplifier design presented here shows promise for future work.

References

(1) Michael Faraday, "On a Peculiar Class of Acoustical Figures, and on Certain Forms Assumed by Groups of Particles upon Vibrating Elastic Surfaces", Phil. Trans. Royal Society London, 121 (299 - 340), 1831.

(2) John William Strutt, Lord Rayleigh, "On the Crispations of Fluid Resting upon a Vibrating Support", Phil. Mag., Series 5, 24, Issue 147 (145 - 159), 1883.

(3) W.W. Mumford, "Some Notes on the History of Parametric Transducers", Proc. IRE, 48 (848 - 853), 1960.

(4) J.M. Manley and H.E. Rowe, "Some General Properties of Nonlinear Elements. I. General Energy Relations", Proc. IRE, 44 (904 - 913), 1956.

(5) William H. Louisell, Coupled Mode and Parametric Electronics, (Wiley, New York), 1960.

(6) L.A. Blackwell and K.L. Kotzebue, Semiconductor Diode Parametric Amplifiers, (Prentice-Hall, Englewood Cliffs), 1961.

(7) M. Uenohara, "Noise Consideration of the Variable Capacitance Parametric Amplifier", Proc. IRE., 48 (169 - 179), 1960.

(8) H. Heffner and G. Wade, "Gain, Bandwidth and Noise Characteristics of the Variable Parameter Amplifier" J. Appl. Phys., 29 (1321 - 1331), 1959.

(9) M. Uenohara, et. al., "4-gc Parametric Amplifier for Satellite Communication Ground Station Receiver", Bell Syst. Tech. J., 42 (1887 - 1908), 1963.

(10) E. Brenner and M. Javid, Analysis of Electric Circuits, (McGraw-Hill, New York), 1959.

(11) Walter E. Dahlke (NSF Senior Visiting Professor of E.E.), Lecture notes on Theory of Noise and Noisy Networks, (Lehigh University), 1964. unpub.

(12) K. Kurokawa and M. Uenohara, "Minimum Noise Figure of the Variable-Capacitance Amplifier", Bell Syst. Tech. J., 40 (695 - 722), 1961.

(13) H.T. Friis, "Noise Figure of Radio Receivers", Proc. IRE, 32 (419 - 422), 1944.

(14) R. Bateman and W. Bain "New Thresholds in VHF and UHF Reception -- The World Below KTB", QST, 42, No. 12 (30 et. seq.), 1958.

(15) S. Ramo and J.R. Whinnery, Fields and Waves in Modern Radio", (Wiley, New York), 2nd. Ed., 1953.

(16) D. Leenov, private communication.

(17) Harvard University Computing Laboratory, Tables of the Bessel Functions of the First Kind of Orders Zero and One, (Harvard Press, Cambridge), 1947.

(18) G.C. Francis and V. Woodward, Tables of Ordinary Bessel Functions of the Second Kind of Orders 0 Through 9, (U.S. Army Ballistic Research Laboratories, Report No. 1197), 1963.

(19) K. Kurokawa, "On the Use of Passive Measurements for the Adjustment of Variable-Capacitance Amplifiers", Bell Syst. Tech. J., 41 (361 - 381), 1962.

(20) W.O. Troetschel and H.J. Heuer, "A Parametric Amplifier for 1296 Mc.", QST, 45, No. 1 (13 et. seq), 1961.

(21) K.L. Kotzebue, "Optimum Noise Performance of Parametric Amplifiers", Proc. IRE, 48 (1324 - 1325), 1960.

(22) S.T. Fisher, "Theory of Single-Resonance Parametric Amplifiers", Proc. IRE, 48 (1227 - 1232), 1960.

(23) F.A. Brand, W.G. Matthei, and T. Saad, "The Reactatron -- A Low-Noise, Semiconductor Diode, Microwave Amplifier", Proc. IRE, 47 (42 - 44), 1959.

(24) R. Bateman and W. Bain, "New Thresholds in VHF and UHF Reception -- Devices and Diodes", QST, 43, No. 1 (11 et. seq.), 1959.

(25) R. Bateman and W. Bain, "New Thresholds in VHF and UHF Reception -- Circuit Theory and Diode Details", QST, 43, No. 2 (28 et. seq.), 1959.

(26) R. Bateman and W. Bain, "New Thresholds in VHF and UHF Reception -- Practical Results", QST, 43, No. 3 (35 et. seq.), 1959.

(27) H. E. Rowe, "Some General Properties of Nonlinear Elements. II. Small Signal Theory", Proc. IRE, 46 (850 - 860), 1958.

Vita

Richard Alan Stanley was born 30 June 1941 in New Haven, Connecticut, to Norman R. and Laura M. Stanley. He was raised on the Southern Connecticut seacoast, attending Woodmont and Nichols Elementary Schools, and Middlebrook Junior High School. In June of 1959, he was graduated valedictorian of a class of 435 from Warren G. Harding High School, Bridgeport, Connecticut. The following September, he was enrolled at Lehigh University, where he received the degree of Bachelor of Science in Electrical Engineering in June 1963, with Honors and College Honors. In September 1963 he was enrolled as National Aeronautics and Space Administration Graduate Fellow in Electrical Engineering at Lehigh University.

Mr. Stanley is a member of Tau Beta Pi, Eta Kappa Nu, Phi Eta Sigma, and the Institute of Electrical and Electronics Engineers. As an undergraduate, he was a General Motors Scholar. He is a commissioned Second Lieutenant in the United States Army Signal Corps.

Professionally, Mr. Stanley has worked as an engineer's assistant for the Bryant Electric Company, Bridgeport, Connecticut; and in an engineering capacity for the AC Spark Plug Division, General Motors Corporation, Milwaukee, Wisconsin, where he was involved in work on Project APOLLO guidance system checkout equipment.